



Critical analysis of polyindole and its composites in supercapacitor application

Harish Mudila^{1,2} · Parteek Prasher³ · Mukesh Kumar⁴ · Anil Kumar² · M. G. H. Zaidi¹ · Amit Kumar⁵

Received: 19 March 2019 / Accepted: 28 June 2019 / Published online: 2 July 2019
© The Author(s) 2019

Abstract

Polyindole-based hybrid composites are being recognized as a promising candidate to be used in energy storage field along with other conjugated organic polymers. Polyindoles themselves are affected with low electrical and electrochemical conductivity; nevertheless, high redox activity, tunable electrical conductivity, significant thermal stability, slow degradation rate, and possible blending property give them upper hand to be used as a good contender. Certain factors viz. electrolyte, concentration, morphology, pH, temperature, etc., are major components affecting performance of Polyindole and its composites. This assessment recapitulates the position of Polyindole and its hybrid composite to be used as energy harvest material; in addition, this evaluation also pronounces the future aspect of the hybrids.

Keywords Polyindole · Capacitance · Electrochemical synthesis · Charge–discharge · Hybrid composites

Introduction

In recent times, ultracapacitor/supercapacitor had emerged as a prime field of scientific concentration, attributed to the interest of scientists to figure out the behaviour and mechanism of different materials towards charging and discharging, while, on the other hand, generation of ultracapacitor/supercapacitor possess the potential to sort out the current problem of energy storage. Electric double layer capacitors (EDLC) and pseudocapacitors are the two forms in which the electric energy can be stored [1]. The charge in EDLC (Fig. 1) is stored through adsorption mechanism

(non-Faradaic) hence called true capacitors, while pseudocapacitors charge generated are pseudocapacitance arise via redox reaction (Faradic) [2, 3]. The combination of these two generates a hybrid capacitor having properties of wide scan range, high power density, high rate of charge–discharge, and minimum Equivalent Series Resistance (ESR). Advanced research and scientific intelligence had provided numerous materials which are efficient in holding great amount of electrical energy thus to provide the stored energy at the time of prerequisite. However, the rendered energy by the material synthesized depends upon number of factor which defines the suitability of the material to be used as an efficient source of energy.

In the route to develop high class energy storage device, organic conducting polymers (CPs) had find their explicit position [4, 5], which were thought to be electrically insulated till year 1977, when research group of *Hideki Shirakawa* unveils their electrical conducting properties [6]. CPs are considered to be conducting in nature attributed to their rapid redox process which offers pseudocapacitance to be stored by the supercapacitor. However, these CPs (conducting polymer) possess variability in their conductance as they swing in between their two forms, i.e., conduction and insulation [4]. Among variety of CPs, Polypyrrole (PPY), Polyaniline (PANI), Polythiophene (PTH), and Poly(3,4-ethylenedioxythiophene) (PEDOT) are the most explored one owing to their high conductivity (credited to extended π

✉ Harish Mudila
harismudila@gmail.com

✉ Parteek Prasher
parteekprasher4@gmail.com

¹ Department of Chemistry, G.B.P.U.A & T, Pantnagar, Uttarakhand 263145, India

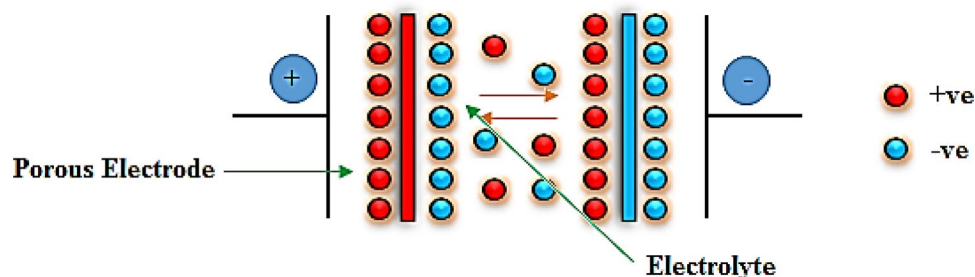
² Department of Chemistry, Lovely Professional University, Punjab 144411, India

³ Department of Chemistry, U.P.E.S, Dehradun, Uttarakhand 248007, India

⁴ Department of Chemistry, Sri Aurobindo College, University of Delhi, Delhi 110017, India

⁵ S.D. Agriculture University, Gujrat 385506, India

Fig. 1 Electric double layer capacitor (EDLC)



conjugated spine), flexibility, quick charge–discharge property, high specific capacitance, synthesis ease, cheapness, and light weight [7]. Apart from these existing properties, the existence of *polarons* and *bipolarons* is must to generate charge carriers [–ve (negative) and +ve (positive) charge] in the polymer backbone [2], *p* and *n* doping can be done for generation of such charge carriers.

In recent years, another CP, named Polyindole (PIN), is being explored and developed as a possible candidate for the electrical energy storage. PIN or Polybenzopyrrole is polymer of Indole and is reported to be synthesized by emulsion polymerization [8], chemical oxidative polymerization [9], electrochemical polymerization [10], microwave-assisted polymerization [11], etc. However, PIN is least studied CP studied for energy storage as compared to others certainly owing to its low electrical and electrochemical conductivity as compared to PPY and PANI by a factor of two [5, 8]. Likewise, other intensively used CP, PIN also suffer from disadvantage like instability, mechanical strain over long cycles, material degradation and loss which, in long time, can even lead to loss in capacity and collapse of capacitor device [7]. PIN is non-planar, light weighted, loosely compact, and arbitrarily oriented polymer leading weak association among the polymer chains leading to low conductivity [12]. The reason behind this mechanical instability and other disadvantage is maximally attributed to structure irregularity in their chain [13]. In spite of this the properties like high redox activity, tunable electrical conductivity, appreciable thermal stability, as well as slow degradation rate make PIN somewhat a considerable material for energy storage studies [14, 15]. To overcome the discussed loopholes, to make PIN technically feasible and to enhance its performance certain modifications in existing polymer are being carried on. In recent times, polymeric scaffolding method is found to act as a prototype for building PIN with reduced heterogeneity in the planar structure and increasing stereoregularity, electrostatic orientation, counter ion supply for better doping, and hence increased conducting properties [16]. These modifications can be brought out by compounding CP with certain other materials (in form of filler or may be a matrix).

This present assessment aimed to cover the investigation on the application of PIN, its modified analogues, and

hybrids as a potential candidate for generation of efficient energy storage material. The authors had tried to summarize the synthesis of PIN, modification in PIN to generate composites, and advantages and disadvantages of PIN as CP. The individual and combine effects of concentration of monomer and filler, morphology and particle size of electroactive material, temperature, type of electrolyte, etc. had been summarized so as to understand their mutual effect on the conducting properties of PIN. Authors believe that this review work will certainly summarize the efforts done by the previous researcher and will be a guiding light for the upcoming research for PIN as a promising candidate in the field of energy storage amongst the existing CPs.

Synthesis of PIN

As discussed in the last section, researchers had synthesized PIN via numerous ways; the various synthetic ways had generated nanosized PIN which can be employed for several applications. The second and third positions in the Indole ring are the sites for coupling where no involvement of the N atom and benzene is observed during polymerization [8]. The effect of substitution on Indole ring and the choice of solvent used in various methods of syntheses play a significant role in overall polymerization of monomer [17]. Apart Soylu et al. had studied the effect of solvents (HClO_4 and BF_3) over the polymerization and conductivity as prepared electroactive material to suggest the effect of position attachment of these to the Indole. They observed that H^+ adds to carbon third of Indole and breaks the conjugation, while BF_3 attaches to nitrogen atom and does not affect the chain conjugation [18]. Few reported polymerization conditions for PIN are tabulated in Table 1.

Emulsion polymerization

This polymerization process is initiated through self-assembly at the interface of two phases, where the organic phase is consisting of monomer and oxidant is present in aqueous phase apart from this certain emulsifier or surfactants which are required for the polymerization process (Scheme 1) [17,

Table 1 Few reported polymerization conditions for PIN

Medium	Oxidizing agents (surfactants)	Refs.
H ₂ O	FeCl ₃ and APS (CTAB, SDS, TW-80)	[8]
HCl	APS (SDS)	[20]
ACN	APS	[44]
H ₂ O, CHCl ₃	FeCl ₃ and APS	[66]
CHCl ₃	FeCl ₃	[36, 48]
H ₂ O, MeOH	CuCl ₂	[34]
EtOH	APS	[44, 78]

[19]. Emulsion polymerization method provides numerous advantages over other method of polymerization. A rapidly polymerized and low polydispersive polymer with high molecular weight can be synthesized with this method, which also can be extracted easily from the reactor owing to its low viscosity.

Nanoform PINs were synthesized by emulsion polymerization technique by number of researchers using variety of surfactants and oxidizing agents. Type of surfactant and oxidizing agent used strongly effect the electrical conductivity of CP. In addition, the preparation of CP with anionic surfactant is much greater as compared to cationic or non-ionic ones owing to their more doping efficiency and small size [8]. Nanosized PIN were generated at room temperature with oxidizing agent [FeCl₃ and ammonium persulphate (APS)] to monomer molar ration of 2.57 in HCl (aq. 0.1 M), the as-prepared nanoparticles were found to have a size of 60.3 ± 10.8 nm [8]. Emulsion polymerized PIN (molecularly imprinted polymer) were synthesized by sonicating ethylene glycol dimethacrylate and TW-60 in water, and the problem of mass transfer was overwhelmed as molecularly imprinted polymer were found to be selective to Indole. The surface area and pore number and size were found to be enhance; also the kinetics of the reaction was found to be of pseudo-second order, while both Langmuir and Freundlich isotherm models were best fitted [20], while non-imprinted PIN

was also prepared by omitting the template of Indole in the polymerization process.

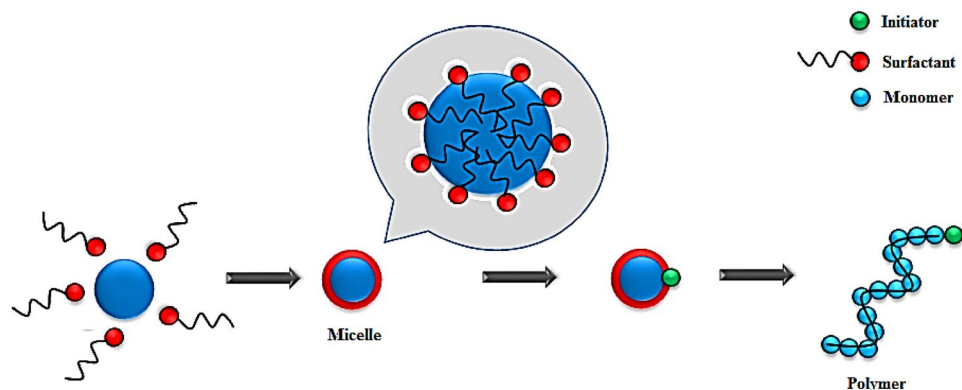
However, this method is affected with certain limitations of presence of traces of emulsifier in final product leading to reduced transparency, final product involves coagulation and with exclusion of aqueous phase (water lowers the yield due to opposite nature); that is why the synthesized polymer could be difficult to yield and expensive also.

Chemical oxidative polymerization

Indole monomer in reaction medium with suitable oxidizing agent and dopant can be carried to polymerization (PIN). Different research groups had employed various oxidizing agents, reaction medium, and dopants for successful synthesis. Apart from the choice of the above three mentioned chemicals, other parameters, viz., concentrations of reagents, reaction temperature, reaction time, and preparatory methods, also determine the percentage of product formation [17, 21, 22].

Equimolar amount of Indole and citric acid were charged in methanol at low temperature (0–5 °C) and then added with CuCl₂; the resulting material was then sonicated for an hour to generate greenish black product [9]. Polymerization of Indole in the presence of FeCl₃ was done on DNA (deoxyribonucleic acid) template by Hassanien et al. [23], and magnitude of templating depends upon non-covalent interaction between the cationic PIN and anionic DNA. Various polymerization combinations of tert-butyl ammonium perchlorate (TBAP), Indole monomer, with Cu(ClO₄)₂·6H₂O oxidant were taken in the presence of Lewis acids like BF₃ and HClO₄, at 5 °C for 24 h [18]. 1:5 (FeCl₃: Indole) was heated at 15 °C for hours with nonstop stirring to generate PIN for Li-ion battery application where PIN was used as cathode [24].

However, this polymerization method is limited with drawbacks like fabrication of complete region-regular polymer is difficult, difficult to limit molecular weight or

Scheme 1 Emulsion polymerization of Indole monomer

dispersity, no control over the polymer end group, and also the purification of final product is not easy.

Electrochemical synthesis

Electrodeposition method is considered to be a new, smooth, and rapid way of polymerizing conducting polymer films that are determined by electrochemical parameters (addition of dopants and hydrophilic/hydrophobic substituents) and the monomer (core structure) to be polymerized (Fig. 2a) [25]. Electrochemical polymerization methods are chiefly employed used in union with three-electrode assembly techniques like potentiostatic, galvanostatic, or potentiodynamic (Fig. 2b) [17, 26]. The advantages of these advance synthetic techniques involve excellent reduction–oxidation activity, and thermal and physical stability of the polymer synthesized and sluggish rate of degradation [17, 25]. As observed, the electrochemically synthesized π -conjugated polymers in ionic solution do show improved lifecycles and rapid cycle switching speeds without considerable material loss [27].

Cyclic voltammetry (CV, 1.2 V) technique was effectively used for polymerization of indole on the surface of Pt (Platinum) in solution containing 0.1 M NaClO₄, the green-coloured precipitate signifies the generated polymer [28]. Boron trifluoride diethyl etherate-assisted electrochemical polymerization of indole and its various

derivatives was carried over stainless steel surface and was ascertained by ¹H-NMR. The amount of polymer deposited on the substrate was effectively controlled by charge provided through the source. The electrothesized polymers generally have benefits like thermal permanence, high redox activity, and sluggish rate of degradation [29]. Derivatives of indole over glassy carbon electrodes were potentiodynamically polymerized. The polymerization process was carried for 25 cycles at the scan of 0.05 V s⁻¹. Fifth and sixth position substituted indole were found to polymerize rapidly as compared to second position substituted indoles, attributed to hindrance produced by the substituent when it is present in pyrrole ring of benzopyrrole [30]. Hydrophobic-fluorinated nanosphere PINs were synthesized from corresponding monomers by potentiostat in 0.1 mol solution of tetrabutylammonium perchlorate dissolved in anhydrous acetonitrile [25]. PIN films were grown over Pt and mild steel/Ni electrodes in 0.2 M indole containing ACN-LiClO₄ (Acrylonitrile–Lithium chlorate) medium. Thus, obtained films were stable, homogeneous, and less porous, which were found to be more stabilized with repeated cycles [31].

However, the electropolymerization is disfavoured by problems like hydrolysis and over-oxidation (polymer got further oxidised at higher anodic potential) which can cut down the electroactivity and conductance of the CP [4].

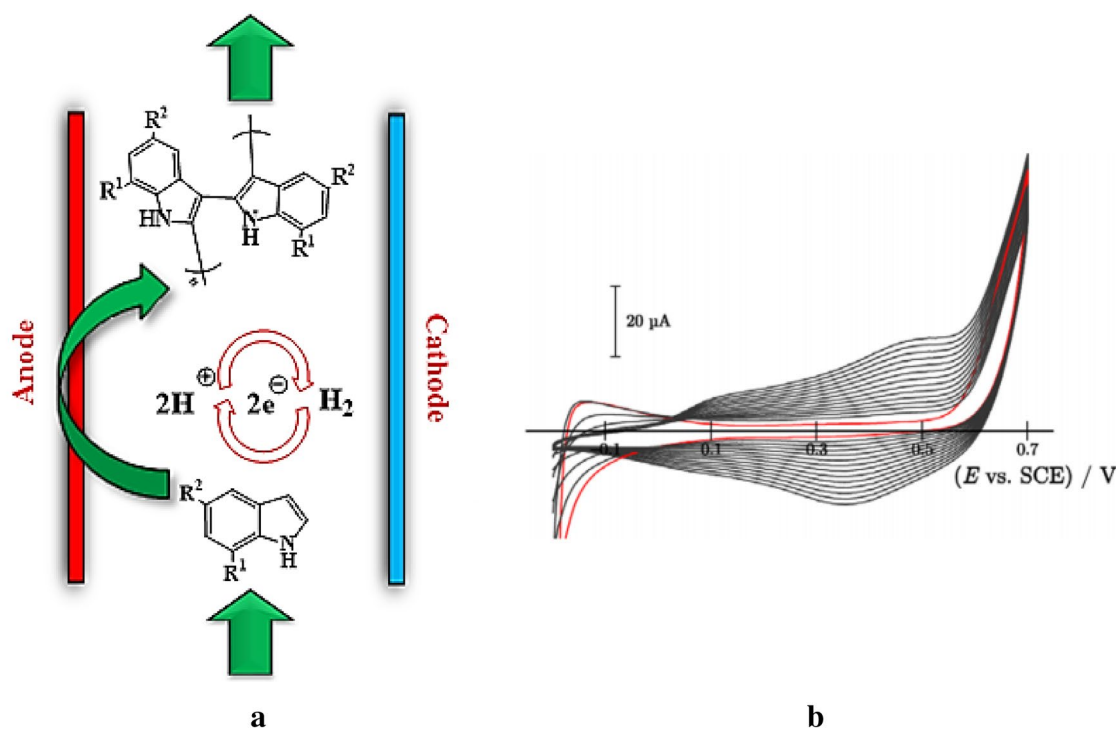


Fig. 2 **a** A systematic representation of electrochemical synthesis; **b** CVs acquired during the electrochemical synthesis of PIN [26]

Synthesis of PIN composite for enhance conductance

As discussed earlier PIN is affected by certain drawbacks like low electrical and electrochemical conductivity, instability, mechanical strain over long cyclic spans, material degradation, etc., which limits the applicability of PIN as an individual potential energy storage material; however, this CP in combination with certain dopants, viz., organic materials and metallic components, is proved as future generation candidate [14, 32, 33].

PIN/metallic (metal oxide) composite

Low electronic conductivity, poor specific conductance, and meagre electrochemical stability during cycling are generally observed for metal oxides, which can be swamped by compositing them with carbon material (carbonaceous polymers) [34]. Thus, it can be assumed that both CP and dopants are complemented by each other's presence. As-synthesized nanosized ZnO [from $\text{Zn}(\text{O}_2\text{CCH}_3)_2$ and $(\text{NH}_4)_2\text{CO}_3$ (1:1) in water and 10% Gum Tragacanth solution] was mixed to monomer with dropwise addition of CuCl_2 and stirred continuous (0–5 °C) to generated conductive PIN/ZnO composites [35]. Sol–gel method was employed for fabrication of conductive PIN/Ce(IV) vanadophosphate by mixing CAN (ammonium ceric nitrate) and sodium vanadate with H_3PO_4 [36]. Binary composite of PIN/ MoS_2 was obtained by adding the suspension of hydrothermally exfoliated MoS_2 to the solution of indole monomer in the presence of APS with continuous stirring at 0 °C for 12 h [37]. Co_3O_4 was electrodeposited to PIN in presence of NaNO_3 and HNO_3 (electrolytes) at 700 mA cm^{-2} where stainless steel and graphite (Gr) acts as cathode and anode, respectively [34]. Bamboo-shaped in situ polymerized PIN/ V_2O_5 nanostructured composites were decorated over activated carbon cloth by ion-exchange column method to provide higher activated surface area and pores [38].

PIN/carbon composite

In situ fabrication of PIN/carboxylated multiwalled carbon nanotube (MWCNT, 5% w/w of monomer) was carried in H_2SO_4 by dropwise addition of APS (oxidizing agent), while interfacial polymerization technique was used having the same composition with vigorous sonication [39]. Monomer:CNT (20:1) was taken by Cai et al. at 0 °C in N_2 environment, CHCl_3 was the solvent with APS used as oxidant and ultrasonicated [14]. A binary composite of PIN/CB was obtained by adding CB (carbon black) to the solution of indole monomer in presence of APS with continuous stirring at 0 °C for 12 h [37].

Electrical and electrochemical performance of PIN

The conductance of PIN among various CP is observed to be less (close to 0.1 S cm^{-1}) owing to their instability, degradation, chain unevenness, etc. However, the properties of dopant (its size and nature) and nature of electrolyte-molecular solvent system can have a discernible impact on the conductance of the subsequent polymer [27]. In addition, in the case of electrochemical storage, the scan rate effects of the current response, with lower rates of scanning the thick diffusion layers, are formed which are responsible for reduced current response while vice versa for high scan rate [34, 37].

In the CPs, due to lack of perpetual dipoles, the charge trapping is found to be difficult; thus, the localized motion acts as electrical dipole under applied electrical field, where the charge carriers are allowed to carry the charge to contiguous sites to produce a network throughout the dimension of the material [40].

Phasuksom and Sirivat [8] claimed synthesized PIN to generate conductivity equivalent to metallic conductors, PIN synthesized by various combinations of surfactants and oxidizing agents renders electrical conductivity of different level. Electrical conductivity of PIN/ FeCl_3 was in the range of $(7.4 \pm 2.9) \times 10^{-4}$ S cm^{-1} to $(1.15 \pm 0.28) \times 10^{-3}$ S cm^{-1} , PIN/APS generates $(5.41 \pm 0.23) \times 10^{-5}$ to $(2.16 \pm 0.31) \times 10^{-4}$ S cm^{-1} . However, the conductivity was enhanced (14.56 ± 2.39 S cm^{-1}) by doping with HClO_4 , but this condition is hampered when doping is excessive which leads to reduction of +ve charge N in the polymer backbone. Similarly, PIN synthesized with SDS (sodium dodecyl sulfate) as surfactant was found to generate more electrical conductivity as compared to CTAB (Cetyltrimethylammonium bromide) and TW-80. While the synthesized PIN with APS by Park et al. [41] was having electrical conductivity of 5.5×10^{-5} S cm^{-1} which subsequently decrease after de-doping. PIN synthesized in $\text{Cu}(\text{ClO}_4)_2 \cdot 6\text{H}_2\text{O}$ generates low level of electrical conductivity (6.0×10^{-7} S cm^{-1}) in protonic acidic solution (HClO_4) due to broken polymer chain, while, in the presence of BF_3 , no polymer backbone is ruptured resulting in higher electrical conductivity (4.6×10^{-4} S cm^{-1}) of synthesized polymer [18]. Electropolymerized synthesized PIN were objected to four-point probe for ascertaining the conductivity, the conductance was found to be low as 0.03 mS cm^{-1} [42]. PIN was polymerized over gold electrode in ionic solution [BMIm] $[\text{BF}_4^-]$ (1-butyl-3-methylimidazolium tetrafluoroborate) or [BMIm] $[\text{PF}_6^-]$ (1-butyl-3-methylimidazolium hexafluorophosphate) and were compared to LiClO_4/I . CV of obtained polymerised material (PIN) demonstrates the higher electrochemical activity and electropolymerization of PIN synthesized in [BMIm] $[\text{BF}_4^-]$ or [BMIm] $[\text{PF}_6^-]$

compared to $\text{LiClO}_4/\text{CAN}$ [27]. However, the conductivity of PIN in CAN was higher than PIN electropolymerized in [BMIm] $[\text{BF}_4^-]$ and [BMIm] $[\text{PF}_6^-]$ by an order of 0.8 and 0.4, respectively.

PIN prepared by Cai et al. was found to generate an electrical conductivity of 0.086 S cm^{-1} [14], while PIN nanofibers prepared by Zhijiang et al. generate electrical conductivity of 0.24 S cm^{-1} [43]. PIN doped with H_2SO_4 ion over Li was studied for cell purpose by Cai and Yang, and these cells demonstrate excellent cyclic behaviour (best discharge capacity and saturation after 15 cycles), which retained 98% after 5000 cycles [31]. The DC conductivity of PIN was enhanced from 0.15 to 2.0 S cm^{-1} on charging. PIN-PC-15-9 [44] was found to have electrical conductivity of $22. \text{ S cm}^{-1}$.

Supercapacitor electrode materials (CPs) are often strike back with lack of steadiness during repetitive redox processes which diminished the initial performance, and thus, excellent cyclability is found to be a crucial component for the supercapacitor material [45]. For studying electrochemical behaviour of CPs, appropriate solvents and electrolytes required. CV and GCD (galvanostatic charge–discharge) are studied for the specific and gravimetric capacitance of the materials [17]. The electrochemical behaviour of the CP films depends upon the dopant anion used in polymerization process; more basic anion will generate inferior electroactivity by producing thin insulating film, hence restricting the polymerization process.

PIN cathode having high charge density and fast charging and delayed discharging property was employed for Li-ion battery application. The as-fabricated cell (PIN as cathode and Li as anode) rendered specific capacity $80\text{--}70 \text{ mAh g}^{-1}$ at discharge current densities of $10\text{--}10^3 \text{ A m}^{-2}$. The cell maintains 87% of its capacity after its repeated 5000–30,000 cycles (2–7% drop) depicting its fast charge–discharge and excellent cyclic behaviour [24]. CV studies of fluorinated PIN synthesized by Chagas et al. show the low redox peak for the synthesized polymers due to low conductivity of PIN [25]; however, the material deposition was also less attributed to formation of oligomers. Majumdar et al. describe the occurrence of redox peaks for PIN which may be attributed to the generation of polycationic state due to delocalized polarons in the polymer chain hence leading to storage of faradic charge, with specific capacitance of 112 F g^{-1} , energy density of 2.11 Wh kg^{-1} , and power density of 135 Wh kg^{-1} at 1 A g^{-1} [37]. PIN was found to have a specific capacitance and specific volumetric capacitance of 343.2 F g^{-1} and 137.3 F cm^{-3} in aqueous system, while 381.9 F g^{-1} and 152.8 F cm^{-3} in non-aqueous system [14]. Fifth, sixth, and seventh positions of carboxylic acid monosubstituted PINs' (PINC) nanowires were subjected to electrochemical conductance studies by Zhou et al., to produce specific capacitance of 364, 384, and 429 F g^{-1} suggested by CV curves. Similar results were shown by GCD (355,

383, and 430 F g^{-1}) at current density of 2.5 A g^{-1} . Symmetric anodic and cathodic charges demonstrate brilliant efficiency and cyclability of the as-prepared materials attributed to their high adsorptive capacity and facile ion diffusion [46]. PIN-derived porous carbon materials (PIN-PC) at $700\text{--}900 \text{ }^\circ\text{C}$ and $7\text{--}20 \text{ M KOH}$ solution were synthesized by Wu et al., which were found to have appreciable surface area of $2238 \text{ m}^2 \text{ g}^{-1}$ with a high specific capacitance and energy density (15 Wh kg^{-1}) at 0.2 A g^{-1} [44]. Nanomaterial at 7 M KOH and $900 \text{ }^\circ\text{C}$ was observed to have better CV compared to other prepared materials. Researcher found that, with increasing concentration ($7\text{--}15 \text{ M}$) of electrolyte, the electroactive material's pore size and specific area are enlarged which leads to amended specific capacitance, but, however, decrease in specific capacitance at 20 M KOH was encountered due to decrease in content of N, O in specific area. Electrochemical investigations of electrospun PIN nanowires reveal the specific capacitance values of 238 F g^{-1} (at 1.0 A g^{-1} , CV) and 155 F g^{-1} (5 mV s^{-1} , GCD) [6].

Conductivity of PIN composites

It is well known that the conductivity of a conducting polymer can be drastically improved through doping with other ions or species [24], to generate binary or ternary composites. Both electrical and electrochemical conductivities are observed to get augmented with addition of variety of components in the matrix of CPs up to a certain limit only [33, 47]. Comparative analysis of PIN, its derivatives, and PIN-based composites are tabulated in Tables 2 and 3.

PIN/metal (metal oxide) composite

Metal oxide/conducting polymer-based pseudocapacitors generate high specific capacitance with a drawback of short cycling life, whereas carbon materials EDLCs hold great power density and stability, and generate rapid charge–discharge rate with low specific capacitance [47]. Composites of metal oxides with conductive polymers or carbonaceous materials are employed as supercapacitors certainly attributed to synergistic effects owing to merits, such as high power and energy density, with exceptional recyclability and low degradation of composite material. Metal oxides are environment benign and observed to have high theoretical electrochemical capacitance and performance [38, 47], owing to their multivalent oxidation states.

PIN/CdSe composites were studied by universal power law and observed to comprise of higher order of activation energies and low level of electrical conductivity in comparison to the undoped polymer, which may be attributed to coordination among unpaired electrons of nitrogen of polymer and empty orbital of CdSe after doping which

Table 2 Capacitance analysis of PIN and its derivatives

Electrode material	Electrolyte	Highest capacitance observed (F/g)		Current density	Power density (W kg ⁻¹)	Energy density (Wh kg ⁻¹)	Durability	Refs.
		CV	GCD					
PIN	1 M KOH	21.89	–	0.1 V/s	–	–	96% after 50 cycles	[32]
PIN	1 M KOH	24.48	–	0.1 V/s	36	1.0	–	[5]
7-PINC	1 M H ₂ SO ₄	430	429	2.5 A g ⁻¹	1125	48.3	96% after 1000 cycles	[46]
PIN-PC-15-9	7 M KOH	328	293	1.0 A g ⁻¹	120	15	91% after 10,000 cycles	[44]
PIN	1 M H ₂ SO ₄	238	155	1.0 A g ⁻¹	–	–	–	[6]
5-PINC	1 M H ₂ SO ₄	239.1	232.2	5.0 A g ⁻¹	2900	43	89.9% after 1000 cycles	[77]
PIN	1 M KCl	49	46.87	2.5 A g ⁻¹	–	–	96% after 2000 cycles	[56]
PIN	1 M H ₂ SO ₄	–	117	1.0 A g ⁻¹	2.6	–	73.3% after 5000 cycles	[33]
5-PCIN	1 M H ₂ SO ₄	336	–	2.4 A g ⁻¹	190	23	70% after 1000 cycles	[45]
PIN	1 M H ₂ SO ₄	198	–	2.0 mV s ⁻¹	–	–	–	[78]
PIN	1 M KCl	114	–	2.0 A g ⁻¹	–	–	–	[59]

Table 3 A tabular comparison of PIN composites reported for supercapacitor application

Electrode material	Electrolyte	Capacitance (F/g)		Current density	Power density (W kg ⁻¹)	Energy density (Wh kg ⁻¹)	Durability	Refs.
		CV	GCD					
PIN/V ₂ O ₅	5 M LiNO ₃	535.3	275.5	1.0 A g ⁻¹	900	38.7	91.1% after 5000 cycles	[38]
PIN/MnO ₂	0.5 M Na ₂ SO ₄	221.3	201.6	10 mV s ⁻¹	–	–	73.70% after 5000 cycles	[47]
PIN/MnO ₂ /rGO	0.5 M Na ₂ SO ₄	522.5	448.5	10 mV s ⁻¹	–	–	97.65% after 5000 cycles	[47]
PIN/GO	1 M KOH	399.9	–	–	–	–	99% after 50 cycles	[32]
PIN/Graphene	1 M KOH	389.2	–	–	512	13.51	98.6% after 1000 cycles	[5]
PIN/CNT	1 M H ₂ SO ₄	521	476	1.0 A g ⁻¹	1139	11.44	95% after 2000 cycles	[6]
PIN/CNT/Co ₃ O ₄	3 M NaOH and PVA/NaOH gel	442.5	–	1.0 A g ⁻¹	400	42.9	24.5% after 5000 cycles and 90.2% after 5000 cycles	[58]
PIN/CNTs/RGO	1 M KCl	383	–	1.0 A g ⁻¹	–	–	88.79% after 3000 cycles	[76]
PIN/CNTs	1 M KCl	196	–	1.0 A g ⁻¹	–	–	71.78% after 3000 cycles	[76]
PIN/Hb	1 M KOH	294	–	0.1 V/s	–	–	98% after 1000 cycles	[49]
PIN/h-NCS	1 M H ₂ SO ₄	397	–	1.0 A g ⁻¹	2499	11.38	95.7% after 5000 cycles	[51]
PIN/MWCNT	1 M KCl	206	203	2.5 A g ⁻¹	–	–	96% after 2000 cycles	[56]
PIN/nanoclay	1 M KCl	73	65.62	2.5 A g ⁻¹	–	–	96% after 2000 cycles	[56]
PIN/MWCNT/nanoclay	1 M KCl	533	500	2.5 A g ⁻¹	1066	47	96% after 2000 cycles	[56]
PIN/Nd ₂ O ₃	1 M H ₂ SO ₄	516	401	1.0 A g ⁻¹	115	8.91	95% after 5000 cycles	[33]
5-PINC/PEDOT	1 M H ₂ SO ₄	295.7	285.2	5 A g ⁻¹	2900	52.4	95% after 1000 cycles	[77]
PIN/CNT	1 M KCl	163	–	2.0 A g ⁻¹	–	–	–	[59]
PIN/CNT/α-MnO ₂	1 M KCl	421	–	2.0 A g ⁻¹	800	37	92.1% after 5000 cycles	[59]
PIN/Co ₃ O ₄	1 M KOH	1805	–	2 A g ⁻¹	–	–	82% after 1000 cycles	[34]

restrict the free movement of charge carrier [48]. PIN/ZnO nanocomposite prepared by Handore et al. was subjected to four-probe methods at room temperature for electrical conductivity review. The bulk composite (4.4×10^{-6} S cm⁻¹) and nanoform (1.7×10^{-6} S cm⁻¹) were observed to have higher conductance as compared to the CP alone

1.5×10^{-7} – 2.8×10^{-6} S cm⁻¹ when K₂S₂O₈ and CuCl₂ were used as oxidant, respectively [35]. PIN/Ce(IV) vanadophosphate tablets synthesized via sol–gel method were found to have electrical conductivity of 5.5×10^{-2} S cm⁻¹ when subjected to four-probe assembly [36] and is proposed to be used in semiconductive devices (at < 130 °C).

Composite of PIN/Co₃O₄ prepared by Raj et al. [34] exhibits the similar redox peaks as of pristine Co₃O₄ but with a shift due to presence of PIN, presenting the combination of EDL (electric double layer) and pseudocapacitance of the composite prepared. The charge–discharge properties were symmetric with specific capacitance of 1805 F g⁻¹ which was maintained at even high current density and long cycles, certainly attributed to synergetic relation between the two (Fig. 3a). As-grown PIN/V₂O₅ [38] on activated carbon cloth shows good recyclability investigated by CV and GCD. The distorted-rectangular CV and symmetrical, non-linear charge–discharge suggests pseudocapacitive behaviour of the as-prepared nanomaterial. Nyquist plots indicate low ohmic resistance (1.1 Ω) and charge transfer resistance (7.6 Ω) for the nanocomposite, and, thus, high conductance and low resistance, while the energy and power density of 32.6 Wh kg⁻¹ and 18 kW kg⁻¹ were calculated for the nanocomposite.

Khathi et al. had presented haemoglobin (Hb)/PIN as electrochemical supercapacitor, which shows continuous increment of specific capacitance with increasing Hb ratio. These results could be because of the development of conjugates amongst –COOH of Hb and 2° amine of PIN, which not only

augment the active surface sites, but also torrent the electron transfer between the anodic and cathodic zones [49]. PIN/Fe-porphyrin, hybrid material was in situ synthesized for studying electrochemical and electrical performance. The flower-like arrangement of the composite material was found to have significant effect on electronic and electroactive properties of the material. The Kelvin probe force microscope (KPFM) studies shows variances in potential contrasts of PIN after composite formation which are associated with change in electrical properties due to lowering of highest occupied molecular orbital (HOMO). The synergetic relation between the Fe-porphyrin and CP induces charge transfer as compared to pure CP, and thus, high current density and charge mobility were originated after hybrid formation (Fig. 4). The ideality factor ($\eta = 2.1$) depends upon intrinsic mobility (μ_h), saturation current density (J_0), and barrier height (Φ_B), and shows deviation from ideal diode [50].

–NCS (nitrogen-doped carbon spheres)-doped PIN prepared by Majumder et al. demonstrates distorted quasi-rectangular voltammogram (of simple *h*-NCS), to store energy as pseudocapacitor indicating high redox property, but this CV voltammogram shrinks with increasing PIN in the composite, and hence, limiting the surface area and by

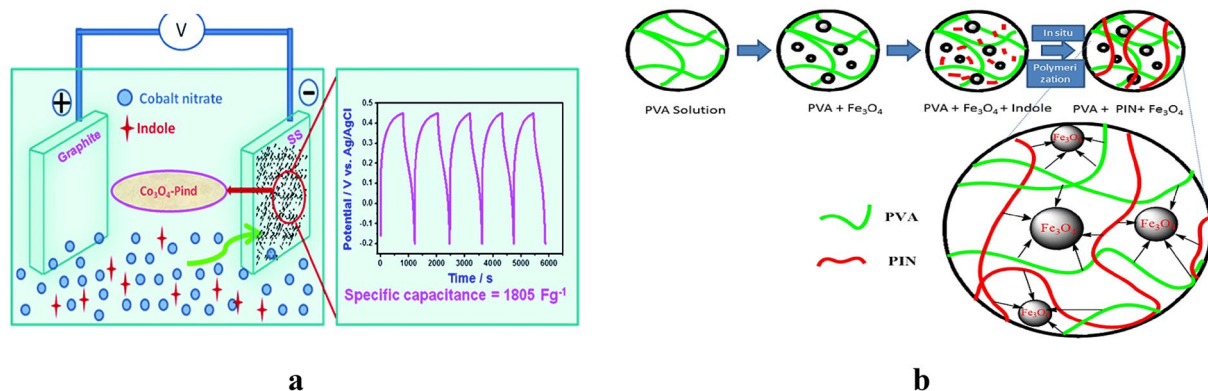
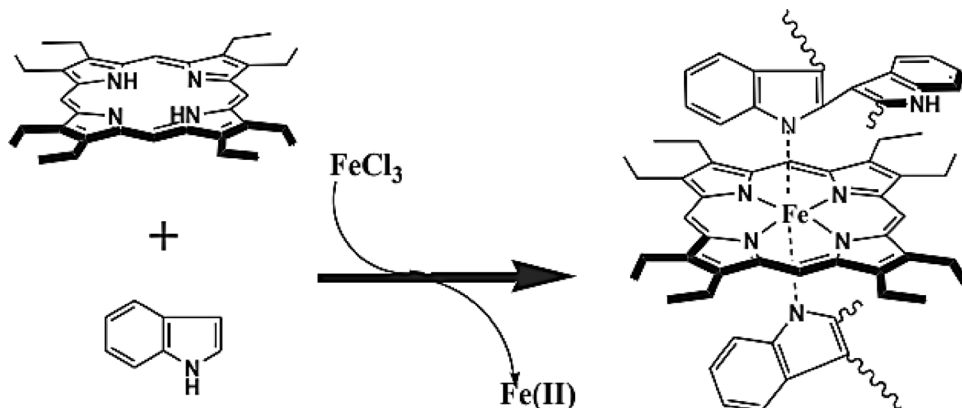


Fig. 3 Graphical representation of PIN composite and its charge–discharge curve (a) [34]; graphical representation of in situ fabrication of PIN composite (b) [13]

Fig. 4 Interaction mechanism between PIN/Fe and porphyrin [50]



blocking the pores (decreasing size and volume) resisting the drift of ions and charge [51], similar result was observed in case of GCD. Majumder et al. incorporate rare earth metal oxides (Nd, Gd, and Yb) in the matrix of PIN (ultrasonicated) to enhance electrochemical supercapacitance of the composites. PIN/Gd₂O₃ and PIN/Yb₂O₃ were found to have non-rectangular CV loop which demonstrate their charge storage via faradic reactions. While PIN/Nd₂O₃ composite was found to have increase CV area and capacitance (which decrease with increasing ratio of Nd₂O₃), this is attributed to lanthanide contraction and low bandgap of Nd₂O₃ [33]. Rajasudha et al., Rajasudha et al., and Rajasudha et al. synthesized and characterized PIN/NiO, PIN/ZnO, and PIN/CuO, composite, ionic conductive studies which were done for the prepared composites; the impedance diagram shows the semicircle under the real coordinate, the composite was found to exhibit high conductivity at higher temperatures due to free voids which enhance mobility of the charge carriers, the composite loaded with specific amount of monomer (0.7, 0.5, and 0.5 g) to 1 g of metal oxide (NiO, ZnO, and CuO, respectively) to bestow highest electrical conductivity [2.6×10^{-4} , 4.4×10^{-7} , and 1.9×10^{-5} S cm⁻¹ at 45, 50 °C, and room temperature (RT)] [52–54]. The increase in the conductivity was observed with increased amount of polymer which was further decreased after a critical limit due to restricted movement of charge carrier (Li⁺) in the amorphous CP. The ionic conduction follows the Arrhenius model which suggests the activation energy to be decreased up to a specific critical limit of polymer in the composites. Similar result was obtained for PIN/Fe₂O₃ composites [55].

PIN/carbonaceous composite

I–*V* curve method was employed by Cai et al. [14], for studying electrical conductivity of PIN/CNT composites (Fig. 3b). The electrical conductance was remarkably enhanced by incorporating CNT into the PIN matrix certainly attributed to CNT's high conductivity and interaction between the two components, hence supporting the charge transfer process, also confirmed by electrochemical impedance spectroscopy (EIS) studies (shows less resistance in composite as compared to PIN).

PIN/CNT composites prepared by Cai et al. show a specific capacitance of 520.8 and 555.6 F g⁻¹ in aqueous and non-aqueous system, respectively, at lower current density, which was 45–50% higher than PIN. These results were credited to evenly distributed nanostructure which offers high interface to electrolyte with matrix and reduces the diffusion distance. However, the increase current density shows negative effect on capacitance, generating the reduction to 317.3 F g⁻¹ and 363.4 F g⁻¹. The material was found to have good electrocyclability after 5000 cycles (8.7% loss) in both aqueous and non-aqueous electrolytes [14]. The PIN/

CNT electrospun nanofibers were observed to have improved specific capacitance data of 521 F g⁻¹ (at 5 mV s⁻¹, CV) and 476 F g⁻¹ (1.0 A g⁻¹, GCD); this CNT addition permits porous and 3D nanofiber morph which enables broader redox peaks and enhanced charge–discharge time compared to PIN [6]. Mesoporous CNT/PIN composites in the presence of nanoclay were fabricated via in situ and ex situ route by Oraon et al. [56]. In situ incorporation of nanoclay layers enables the composite for higher energy storage with good power density (1066 W kg⁻¹) and energy density (47 Wh kg⁻¹). Nanoclay decreases the entanglement density of CNT and generates electroactive surface for charge conduction, which was found to be higher in in situ addition.

CB attributes to the formation of EDL where rectangular CV with no redox peak was obtained for PIN/CB composite [37], also inferred from GCD studies. The as-prepared composite shows specific capacitance of 193 F g⁻¹. Mudila et al. incorporate GO (5–20% w/w) to Indole which was polymerised via surfactant (CTAB)-assisted dilute polymerization method with FeCl₃. The as-prepared nanocomposite was found to have an appreciable specific capacitance [32]. Electrospun PIN/CB [in polyvinyl alcohol, (PVA)] conducting nano-fibrils over stainless steel spun textile yarn (SS-TY) were prepared by Tebyetekerwa et al. [57] PIN with higher load of CB in the matrix was observed to render higher areal and linear capacitance of 8.79 mF cm⁻² and 2.76 mF cm⁻¹ at 50 mV s⁻¹, respectively (quasi-rectangular CV), owing to synergistic influence of nano-fibrous PIN and CB. EIS studies (straight graphical lines) for PIN/CB with highest composition of filler show significant ion diffusion and hence better electrochemical performance with ESR value of 1.1 kΩ cm². The Ragone plot for the prepared material shows comparable energy and power density with the existing research material such as Gr/carbon fiber, Gr porous Gr fiber, mesoporous carbon/MWCNT, etc.

Green approach for fabrication of PIN/graphene nanocomposites was employed by Mudila et al. [5], and graphene (3–9% w/w) was dispersed into in situ polymerised Indole under supercritical condition using CO₂. Specific capacitance of 389.17 F g⁻¹ was generated from 9% w/w composite at scan rate of 0.001 V s⁻¹ with corresponding energy and power density of 13.51 Wh kg⁻¹ and 511.95 W kg⁻¹, respectively.

PIN/metal/carbonaceous ternary composites

The ternary composite (PIN/CB/MoS₂) exhibits excellent pseudocapacitor behaviour, which was enhanced by increasing scan rates, and also the gravimetric capacitance was observed to be higher. The charge–discharge time was also observed to be higher to other two binary composite fabricated by Majumder et al. [37]. The as-prepared composite shows specific capacitance of 160 F g⁻¹ as compared

to PIN/CB/MoS₂ ternary composite with 442 F g⁻¹ capacitance. The connected pores enhance surface area rapid ion exchange and enhance the EDL capacity of the composite material. PIN/CNT/Co₃O₄ generates higher specific capacitance as compared to CNT/Co₃O₄ and bare CNT 306.2 and 92.1 F g⁻¹, and the fillers here effectively enrich the surface area and conductivity attributed to fast ion transport [58]. After increase in concentration PIN and Co₃O₄ beyond a critical limit (0.1 g and 0.3 g, respectively), the specific capacitance was decreased owing to internal resistance, agglomeration, and energy loss due to incessant charge discharge. The cyclic stability in gel electrolyte was found to be higher as compared to solution due to two reasons: first, the gel provides confinement of Co₃O₄ and evading the structural destruction of Co₃O₄ and keeping interaction among substrates and electroactive materials during charge discharge; second, PIN layered Co₃O₄ are less probable towards dissolution in the electrolyte (Fig. 5).

A PIN/CNT/ α -MnO₂, ternary composite was fabricated by Purty et al., it was observed that the CNT and MnO₂

serve as excellent components in the matrix of PIN for acting as a supercapacitor. The CNT generates a brilliant interaction with PIN, while α -MnO₂ provides a large surface area and conducting track for the electrons over the PIN surface [59], α -MnO₂ had an oxidation state of +4 which offers an electrostatic interaction with π electrons of benzene rings and lone pair of electrons of N present in PIN. PIN/PVA/ZnFe₂O₄ nanocomposites were fabricated by in situ polymerization of indole in PVA solution (with SDS) with varying ZnFe₂O₄ concentration (3–15 wt %). AC and DC conductivity studied on the as-fabricated nanocomposites, at 10% loading of ZnFe₂O₄ in the matrix, the conductivity was found to be highest due to excellent dispersion of nanoparticles of the filler in the matrix which, in turn, generates the dipoles, while, at 15% loading due to restriction in hopping of charge carrier, the conductivity was found to be diminished. The dielectric studies suggest increase in dielectric constant with concentration of ZnFe₂O₄ (highest at 10% loadings) and decrease with increasing frequencies (10²–10⁶ Hz) due to poor polarized alignment of molecule at greater frequencies [60].

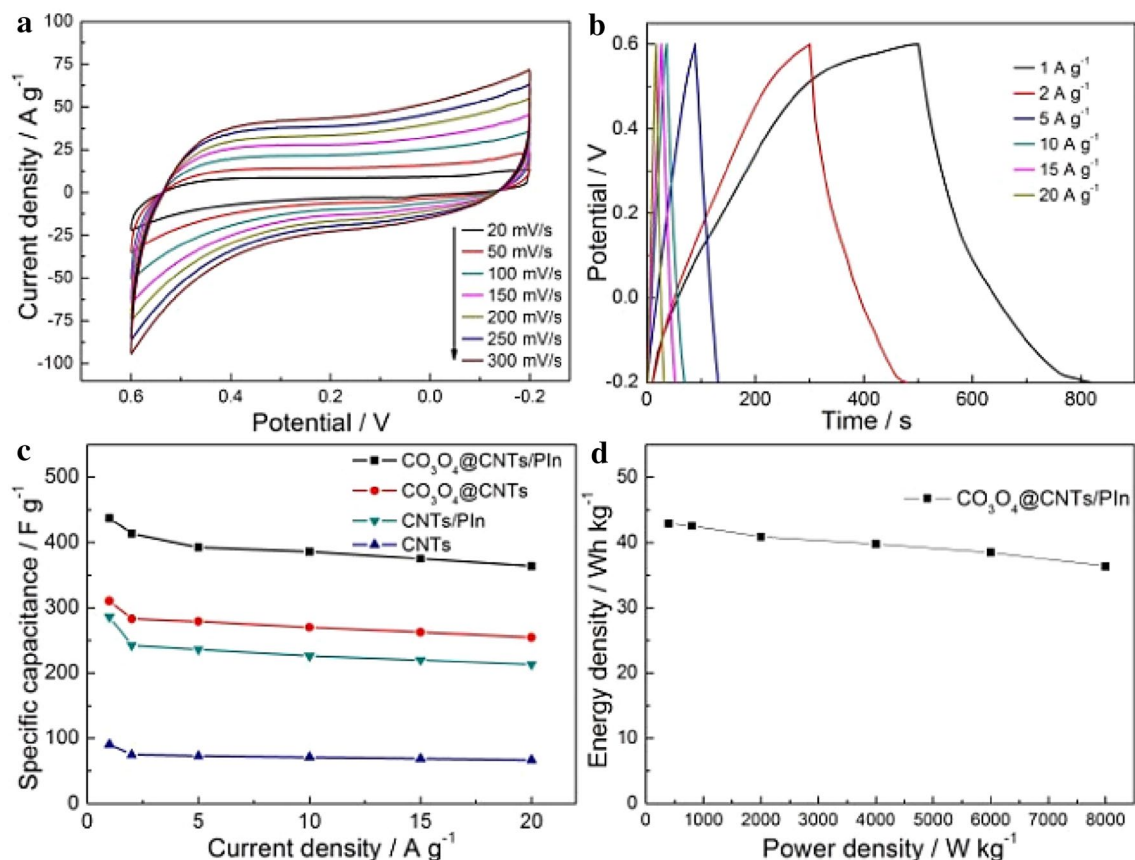


Fig. 5 CVs of PIN/CNT/Co₃O₄; (a) galvanostatic CD of PIN/CNT/Co₃O₄; (b) specific capacitances of CNT, PIN/CNTs, and CNT/Co₃O₄ and PIN/CNT/Co₃O₄; (c) Ragone plots of PIN/CNT/Co₃O₄ [58]

PIN–other CP copolymers

Copolymer of Indole with Thiophene was studied by Sarac et al., 45–300 times higher current and conductivity was displayed; when Thiophene (in 1:1–1:25 ratio) was present in copolymer, this was attributed due to better conjugation between the monomers of the copolymer [42]. PIN was added to polyvinyl acetate (PVAc) to generate PIN/PVAc composite, the composite was further doped with Cu (CuCl_2 , as oxidant in 20–40%), and it was observed that the conductivity of the composite material was proportional to the applied frequency, i.e., from 0.98×10^{-5} to 2.97×10^{-5} S cm^{-1} at 1 kHz and 1 MHz, respectively (for 30% dopant). These results may be attributed to favourable polarization of the present charge transporters and conjugation present in PIN [40]. PIN/PVAc composite oxidised with FeCl_3 (10–50%) was considered for DC conductivity in the temperature range of 35–110 °C. A highest conductivity of 4.5×10^{-6} S cm^{-1} was extracted at 110 °C for 30% composite, while a minimum of 0.38×10^{-6} S cm^{-1} was observed for 50% composition. Increased temperature assists the molecules to overcome the activation energy barrier by orienting the molecules in the direction of applied field this also assist the increased charge transfer thus ensuing high conductivity, while high concentration of oxidant is found to be a barrier in conductivity with restricting the charge carrier in the matrix [61]. PIN/PVAc was prepared with indole monomer added to PVAc solutions in ethanol and FeCl_3 was employed as oxidant by Eraldemir et al. Conductivity studies suggest continuous increase in electrical conductivity (from 1.6×10^{-5} to 4.8×10^{-5} S cm^{-1}) with amount of PIN (13–35%) in PVAc matrix [62].

PIN/PAN composite with varying concentrations (0–2.0% w/v) of PIN in matrix of PAN (Polyacrylonitrile, 10% w/v) was investigated for electrochemical performance. Composition with 1.5% w/v PIN shows uniform morphology [atomic force microscopy, (AFM)], while 1.0% w/v PIN composition shows least diameter fibrous structure [scanning electron microscopy, (SEM)]. Sample with 0.5% w/v PIN was found to have highest specific capacitance due to amorphous and porous fiber with limited PIN concentration (optimum) which provides maximum space for double layer capacitance and movement of ions of electrolyte. Impedance studies for PIN/PAN composite at different ionic concentration ($\text{K}_3\text{Fe}(\text{CN})_6/\text{K}_4\text{Fe}(\text{CN})_6$) provide information on kinetics of electron transfer and diffusion mechanism, where resistance due to charge transfer and electrode resistance were found to decrease with increase in ionic concentration, while electrode capacitance and electrode power were found to increase [63]. PIN and PINCBT [poly(indole-6-carboxylic acid-co-2,2'-bithiophene)] composite were polymerised over ITO (Indium Tin Oxide) surface electrochemically to investigate electrochemical and electrochromic

behaviour. PINCBT films shows doping and de-doping behaviour by its quasi-rectangular CV, while UV (ultraviolet) peaks show bathochromic shift of the peaks in PINCBT (395 nm) as compared to PIN (350 nm) which increases with increasing potential produced due to growing of charge carriers. PINCBT was used as anode, while PEDOT/PSS [poly(styrenesulfonate)] was used as cathode with highest % transmittance of 31% and coloration efficiency of $416.7 \text{ cm}^2 \text{ C}^{-1}$ at 650 nm [64].

Factor effecting conductive performance of PIN and PIN composites

Conductivity of CPs is largely affected by various factors, viz., nature of dopants, process and level of doping, chemical reactivity of dopants, temperature and polymer morphology, crystallinity, etc.

Surface morphology affecting conductance

Well-defined particles size (nano) and morphology of CPs are again found as key factor influencing the pseudocapacitance, and the unstable behaviour of their nanostructure possesses problem in the morphology and, hence, hindered in their performance. It is important to study the effect of micro or nanostructures (grain, tubule, sphere, rods, needles, etc.) on the behaviour of conductance of PIN synthesized via various processes (template or template free) [65]. Chemical synthesis is found to be generating particle of one dimension with amorphous and granular morphology, exhibiting excellent electrical and optoelectronic properties to be used in nanodevices. The microspheres are generated via template method or self-assembly method, which are resulting in hollow microspheres after removal of templates, while polymerization technique like micelle or emulsion are not limited with the same.

Gupta et al. synthesized PIN via interfacial and miscible solvents methods, in case of miscible solvent, stable and unstable micelles produce the hollow microsphere (1–2 μm) and nanorod particle, respectively, while uniform nanorods (diameter > 500 nm) are generated due to interfacial solvent method. Studying the CVs of the PIN polymerised via above two methods shows nearly similar voltammograms with little shift in E_{pa} (oxidation) peak in PIN synthesized via interfacial polymerization method, which is reported to be attributed to higher polymerized chain length and conjugation (Fig. 6.). The shift in the potential peak in CV is owed to sluggish rate of ion diffusion, heterogeneous, and slow electron transfer [65].

PIN-based nanofibers synthesized by Zhijiang et al. were found to have great specific surface area (57–75 $\text{m}^2 \text{ g}^{-1}$) with advantageous application in the field of electrochemical

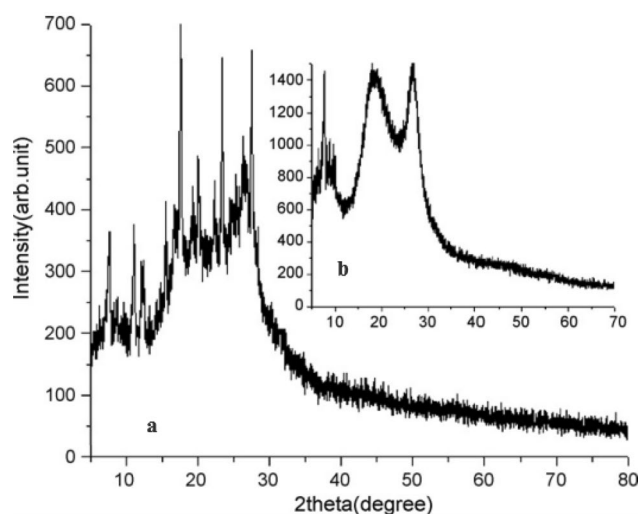


Fig. 6 XRD of nanorod PIN (a) and microsphere PIN (b) [65]

energy storage. This high specific area contributed towards the high charge–discharge performance of the as-synthesized material. PIN of certain viscosity (800 cP) was electrospun, with variable diameter depending upon the applied voltage (16–24 kV) and polymer concentration. With decreasing fiber diameter (347–186 nm), there is increased specific area and hence higher electronic conductivity due to higher charge transfer and alternate electronic paths [66]. PIN/PVAc shows cauliflower morph, and the increasing oxidant (FeCl_3 , 20–40%) concentration effects the morphology of the resulting composites as by altering the rate of polymerization also occurs, besides the AC conductivity of the composite material was observed to increase up to $1.88 \times 10^{-6} \text{ S cm}^{-1}$ at 30% of oxidant added and then considerably decrease on further addition of oxidant [40]. Zhijiang et al. discovered electropolymerized porous PIN nanofibers of smooth, round (250 nm), and low molecular weight (due to high electrical strength and sonication in ACN) which were found to have higher electrical conductivity compared to PIN films. Even in nanofibers, the conductivities were found to be increasing ($0.16\text{--}0.24 \text{ S cm}^{-1}$) with decreasing size (255–768 nm) and increasing surface area. This is owed to the high stretched chain under high electrical impact which allows the neighbouring chains to better interact with other which is higher with decreasing particle diameter [33]. Surfactant had considerable impact on the particle size usually PIN nanoparticle size are considered to be of much smaller size compared to non-surfactant particles. Phasuksom and Sirivat studied the effect of CTAB, SDS, and TW-80 (1:0.05, surfactant to indole) for particle size, use of SDS (anionic) generated least particle size of PIN (due to less electrostatic repulsion compared to CTAB, while $-\text{OH}$ of TW-80 tries to agglomerate the PIN), hence also affecting the morphology and conductance. While the PIN produced

without surfactant was agglomerated with micelle formation, effect of oxidant (FeCl_3 and APS) used also imposed critical effect on the particle size. PIN synthesized in SDS/ FeCl_3 was found to be less agglomerated and having smaller particle size ($60.3 \pm 10.8 \text{ nm}$) compared to the synthesis in SDS/APS ($94.2 \pm 26.4 \text{ nm}$) [8]. Microwave-assisted polymerized indole in KIO_3 is heteronucleated which decreases the energy of activation, reduces size of particles (175 nm), and helps in clustering, better interlinkage, and high electrical conductivity as studied by Tiwari et al. [11]. Studies indicate that not only the intrinsic factor affects the electronic properties but also the geometrical dimensions play the key role for any electroactive material. Decrease in the diameter of polymer nanoparticles/nanofibers produces more compactness and density, thus, providing more conduction routes for charge transference and high conductivity.

Effect of temperature of conductivity

Temperature had significant effect on the conductivity of PIN and its composites, Bhagat and Dhokane, observe increase in a conductivity with increasing temperature for PIN/PVAc composites, attributed to orientation of thermally active PIN and its composite to overcome the conduction band [40]. Perchlorate-doped PIN and self-doped PIN-5-carboxylic acid (5-PINC) were found to have decreased electrical conductivity with time due to the loss of dopant ($> 450 \text{ K}$) and polymer chain conjugation ($> 750 \text{ K}$). Highest conductivity of 3×10^{-2} and $4.5 \times 10^{-2} \text{ S cm}^{-1}$ was obtained for the PIN and self-doped 5-PINC, and with decreasing temperature, the conductivity of both the polymer was reduced by a factor of 4; while, above the 450 K temperature again, there was decrease in conductivity due to loss of perchlorate and carboxylate ion from the corresponding polymers [15]. PIN chains were assumed to decorate uniformly on the Fe_3O_4 particles leading to significant arrangement of matrix filler, the effect of temperature at diverse range was observed by Jayakrishnan et al. At lower temperature (30–100 °C), the DC conductivity of PIN/ Fe_3O_4 nanocomposites was found not to get affected significantly, where the polymer acts as hard polymer. Over 100 °C to 200 °C due to phase change of polymer ($T_g = 128 \text{ °C}$), it was observed that the nanocomposites were generating higher conductivity, credited to the proliferation of numerous conduction tracks generated by the interaction between PIN and Fe_3O_4 nanoparticles [67]. Zhijiang et al. observed significant multi-fold increase in the electrical conductivity ($25\text{--}120 \text{ mAh g}^{-1}$) with increasing temperature (-20 to 60 °C), which they suggested due to the increased electrolyte diffusion in the polymer matrix at higher temperature (Fig. 7) [66].

Similar results were encountered by Rajasudha et al., where increased conductivity with temperature was observed due to hopping procedure of polymer chains, inter-chain ion

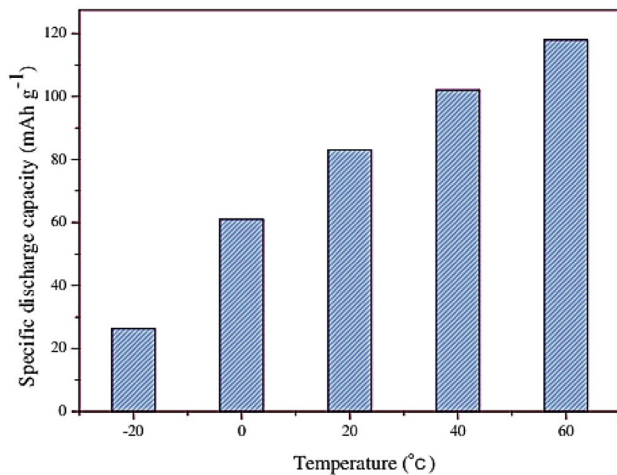


Fig. 7 Effect of temperature variance on the specific discharge capacity of the Li/PIN nanofiber cell [66]

exchange, and segmental movement of polymerised units. The impedance analysis permittivity increases with temperature and decreases with increasing frequency (1 Hz–5 MHz), while the dielectric loss increases with temperature due to restricted segmental mobility of polymeric chain unit owing to increased charge carriers and dopant concentration in the matrix [68]. Concluded that the increasing temperature to a certain limit helps in movement of electrons and also helps in overcoming energy potential barrier, also the increasing temperature generates alternative conducting pathways for the conduction of charge indicating PIN to be acting as better CP at elevated temperature. However, above this critical temperature, the conductivity is affected inversely owing to loss of dopant, etc. Apart increasing temperature also generates alternative conducting pathways for the conduction of charge indicating PIN to be acting as better CP at elevated temperature.

Effect of electrolyte on conduction

Electrolyte type, concentration, solvent viscosity, etc. show a significant role towards the conduction of electricity by certain material. Arjomandi et al. take on the study of electrochemical polymerization of indole in ionic liquids [BMIm] [BF₄⁻], [BMIm] [PF₆⁻], and LiClO₄/CAN. The film growth rate was found to be highest in [BMIm] [BF₄⁻], suggesting the effect of ionic liquid and dopant size. The as-grown PIN films in [BMIm] [BF₄⁻] and LiClO₄/CAN found to have firm capacitance with number of cycles, while performance was twice in case of [BMIm] [BF₄⁻] compared to LiClO₄/CAN. It was observed that the increasing solvent viscosity decreases the polymerization of Indole and, hence, conductivity due to limited mobility of charge carriers [27]. PIN doped with BF₄⁻ ions shows increased electrochemical

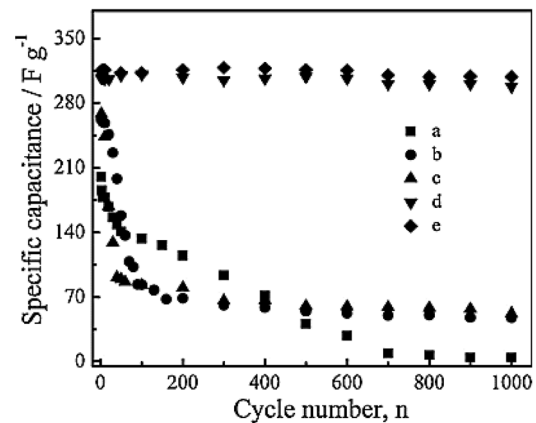


Fig. 8 Effect of electrolytes on the galvanostatic CD of 5-PINC: a ACN/LiClO₄, b Na₂SO₄, c KCl, d H₂SO₄, and e HClO₄ [69]

performance, while doping and de-doping process is affected by the size and surface area of PIN nanofibers [43]. Electrochemical performance of 5-PINC was evaluated in a non-aqueous ACN/LiClO₄ (0.1 M), and four aqueous electrolytes Na₂SO₄, KCl, H₂SO₄, and HClO₄ (0.1 M) by Ma et al., rectangular curves were observed which were maintained at higher scans also, establishing excellent reversible kinetics of the prepared polymer. However, a decrease in specific capacitance (HClO₄ > H₂SO₄ > KCl > Na₂SO₄) was observed at higher scans due to availability of less time for diffusion of anions into the prepared electrode material (Fig. 8). Protonation–deprotonation occurs in the doping and de-doping process which is pH-dependent processes. It was observed that, with decrease in pH, the capacitance performance was improved with broader potential window, signifying that the acidic electrolyte to be better compared to neutral electrolytes. The specific conductance in aqueous electrolytes was found to be higher (301, 305, 325, and 337 F g⁻¹ in Na₂SO₄, KCl, H₂SO₄, and HClO₄, respectively) compared to ACN/LiClO₄ (269 F g⁻¹) at 10 mV s⁻¹. Charge–discharge studies show that the H₂SO₄ and HClO₄ had very minute ohmic loss, solution resistance, and charge transfer resistance. In addition, the cyclability was found to be maximum for HClO₄ (98%) and minimum for ACN/LiClO₄ (2%) after 1000 cycles. Ragone plot displays the highest energy density of 9.6 Wh kg⁻¹ at a power density of 125 W kg⁻¹ [69].

Berkes and Inzelt suggest good oxidation and reduction peaks for PIN and attributed it to entrance and exit (presence) of ClO₄⁻ ions in the polymer film. Apart pH of the electrolyte also controls the performance of the synthesized polymer film, with decreasing H⁺ concentration, it was observed that the conductive behaviour of the PIN diminished, suggesting that the undoped or unprotonated PINs are less or non-conductive [70]. Electrolyte of 1 M H₂SO₄ and LiPF₆ (in EC: DMC, ethylene carbonate, and dimethyl

carbonate) were employed and compared for studying their effect on conductive behaviour of PIN and PIN/CNT composite. Lower shift in the potential value in both the electrolytes signifies the greater extent of conjugation and, hence, greater electrochemical activity for PIN/CNT composite as compared to PIN due to the minimum resistance offered by the evenly distribute CNT in the nanostructure [14].

Effect of concentration of filler towards conductance

The presence of concentration of conducting filler considerably affects the conductance of a CP system, and concentration of this filler to a particular threshold level (percolation limit) generally elevates the required conductance. The conductive network formed between the filler and CP is further affected by particle contact (< 10 nm, between CP and filler), agglomeration tendency, dispersion and polarity of filler, and chain length, size, shape, available surface area, etc. of the CP. Jayakrishnan and Ramesan observed the addition of Fe_3O_4 nanoparticles in PIN/PVA matrix, and it was concluded that further addition of Fe_3O_4 after 10% shows a downfall in the conductivity due to irregular arrangement of the filler nanoparticle in the matrix of the CP, which reduces the hopping of charge (Fig. 9). At the threshold level, the strong conductive network was observed between the CP blend and the filler nanoparticles [13]. DC conductivity was observed to be significantly elevated with the incorporation of magnetite nanoparticles in the PIN matrix, due to collation of the CP with the nanoparticles [12]. Incorporation of filler (Fe_3O_4) nanoparticles to the PIN matrix changes morphology from flaky to rough surfaced which not only assists in polymer matrix formation but also increases the electrical conductance of the system.

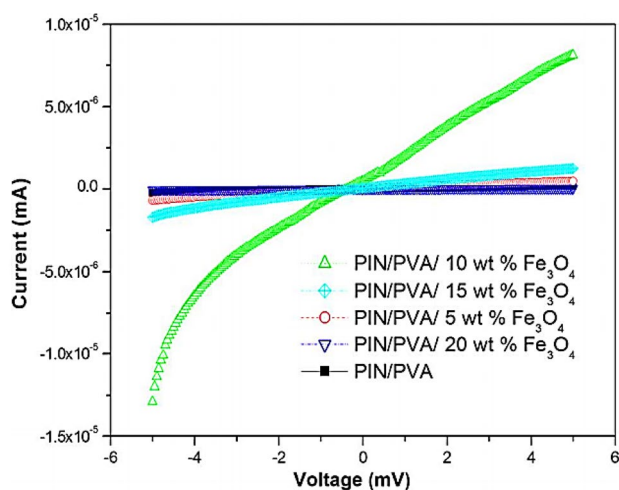


Fig. 9 Effect of Fe_3O_4 nanoparticles on DC conductivity of PIN/PVA blend [13]

PIN due to its good redox activity may be considered to have excellent pseudo capacitive behaviour and is superior to EDLC to store charge. But still, the conductivity is too far less as compared to EDLCs. Therefore, the fillers act as bridging components in the non-conductive shells of PIN thus as to improve the charge conduction and conductivity by better ion transport. Thus, the critical amount of conducting filler just covers the insulating part of the PIN chain.

Surface tension and charge transfer

Surface tension has direct influence on fiber/particle diameter and hence on the electrochemical behaviour. Surface tension behaviour for the composites of PIN/PAN was elucidated by interaction with DMF (dimethyl formamide), and PIN shows its surface active emulsifier behaviour with its increasing concentration and lowers the surface tension. 1.0% w/v PIN (1.0% PIN acting as critical micelle concentration in DMF) was observed to have minimum surface tension and highest fiber charge transfer $121.5 \text{ K}\Omega \text{ cm}^{-2}$. PAN inactivates the surface tension and it diminishes the weak intermolecular interaction between PIN and DMF when added to the matrix (exception being 2.0% w/v PIN in 10% PAN) (Fig. 10) [63].

Effect of surface tension of particle size and, thus, on conductivity was studied on CdSe-doped PIN, and due to high surface tension, CdSe was found to agglomerate in sizes (average size 175 nm) and geometries. Significant differences in the pore size of PIN and CdSe-doped PIN (3:2) was discovered; with increased dopant in the PIN, the particle size and gap in between the particle get decreased due to higher crystallinity achieved. Due to addition of higher amount of CdSe in the PIN matrix, the activation energy is lowered, and electron hopping is easy; however, this

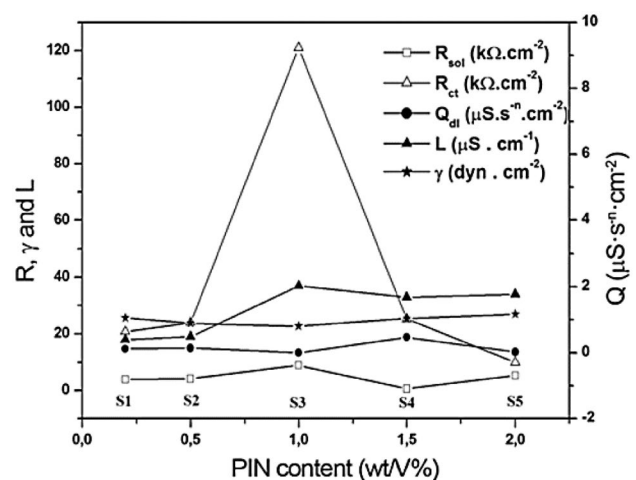


Fig. 10 Relationship of PIN concentration with surface tension (γ) and solution conductivity (L) double layer capacitance (Qdl) [63]

activation energy is lower for PIN as compared to PIN/CdSe composite probably due to coordination between the CP and the CdSe which restrict the movement of charge carrier also due to decrease mobility of π -electron [48].

Effect of bandgap on optical conductivity

Optical band is one of the parameters to judge the optical conductivity of CPs which can be extracted out by plotting photon energy against $ah\nu$. For a semiconducting material, energy bandgap is considered as key feature, so that it can found its application in solar cells, etc. Optical bandgap for PIN with varying concentration of FeCl_3 was determined in 4.6–5.2 eV energy range by Wadtkar and Waghuley. A bandgap of 4.63 eV was observed at 0.6 M FeCl_3 , also the extinction coefficient (absorption loss) was found to be minimum at this concentration, and the maximum optical conductivity of $7.9 \times 10^8 \text{ S}^{-1}$ at 275 nm was observed for the concentration. The result demonstrates that the optical conductivity is affected by the concentration of the dopant (Fig. 11) [71].

Studies done by Nateghi et al. observed 2.17 and 2.0 eV for perchlorate-doped PIN and 5-PICA when the electronic transition between valence and conduction band is electrical dipole allowed with $m = 1/2$ in the following equation:

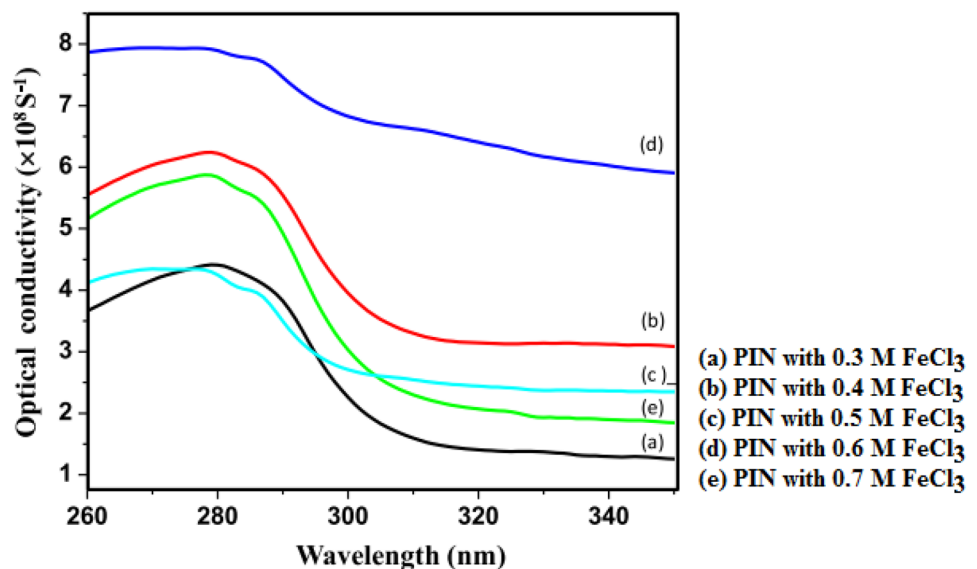
$$(\alpha h\nu) = B(h\nu - E_g)^m, \quad (1)$$

where B is constant, E_g is optical band gap, $h\nu$ is incident photon energy, and α is absorption coefficient.

Increased bandgap in terms of electron withdrawing group attached to PIN was observed which may be due to generation of short length polymer. The extinction coefficient was found to decrease for PIN and increase for 5-PICA with increasing photon energy. Both the electroactive materials

were found to be semiconducting in nature and affected by the value of refractive index and extinction coefficient. The electrical conductivity for the prepared material (PIN and 5-PICA, 8×10^{10} and $15 \times 10^{10} \text{ S m}^{-1}$) was increased with increasing photon energy owed to electron excited by energy of photons [72]. PIN and PIN/ Mn_2O_3 nanoparticles were studied for optical properties by Rejania and Beena, and band edges at 445, 503, and 670 nm were corresponded to PIN, while 330, 420, and 850 nm correspond to $\pi - \pi^*$, $n - \pi^*$, and $n - \pi$ transitions, respectively, for PIN/ Mn_2O_3 nanocomposite. These transitions signify the generation of the polarons in the matrix which further depends upon the concentration of the filler in the matrix of the polymer. A bandgap of 4.4 and 3.3 eV was observed for the CP and PIN/ Mn_2O_3 which further inversely depend upon the particle size of the conductive material [73]. PIN/PVAc composite was studied for its energy bandgap (4.77 eV) and optical properties, and the strongest absorption was observed at 225 nm owing to optical transmission from lower valence band to higher conduction band, while the DC conductivity of the PIN/PVAc composite was $2.45 \times 10^{-7} \text{ S cm}^{-1}$ [74]. Bhagat and Gokhane [61] studied the optical conductivity of PIN/PVAc with varying concentration of FeCl_3 (10–50 wt %) in the UV–Vis range of 200–600 nm, and the composite with 30 wt % FeCl_3 was observed to have highest DC conductivity as well as lowest bandgap of 3.9 eV (4.5 highest for 50 wt %). The loss factor was observed to decrease with increasing photon energy and vice versa, with highest imaginary and real dielectric constant of 16.7 and 295.9 eV at 6.16 eV for 30 wt % composition. They concluded that the material is highly optical conductive when the constituent particles are highly crystalline, small sized (filler), long polymer chained, etc., and apart the material is also affected

Fig. 11 Relation depicting relation between optical conductivity and applied wavelength [71]



by the type and concentration of doping, striking photon energy, etc.

Conduction models

While, in maximum of the CPs, an increase in conductivity with temperature is observed in hopping conductors. Varieties of conduction models are applicable and accounted for different conducting systems or CPs, depending upon specific range of temperature, structure, dimension and crystallinity of CP, type of dopant, and amount and process of doping. Abthagir and Saraswathi 2004 had studied Arrhenius and Mott plots of conductivity for the CPs prepared, and Arrhenius equation is generally employed near room temperature indicating interaction of adjacent charge carriers, whereas Mott model considers that CPs consist of various localized charge centres where the electron hops and wave functions of two adjacent localized charge centre should overlap effectively.

Arrhenius equation:

$$\sigma = \sigma_0 \exp\left(-\frac{E_a}{kT}\right), \quad (2)$$

where σ is optical conductivity, E_a is activation energy, σ_0 is DC conductivity (of pre-exponential factor), k is Boltzmann constant, and T is absolute temperature.

And Mott equation:

$$\sigma = K_0 T^{-1/2} \exp\left[-\left(\frac{T_0}{T}\right)^{1/4}\right], \quad (3)$$

where σ is optical conductivity, K_0 is Mott characteristic conductivity parameter, T is absolute temperature, and T_0 is Mott characteristic temperature.

Thus, the conductivity is treated as function of temperature activated by hopping from various charge hubs and inclines to nil with temperature. The slope of Arrhenius plot produces an activation energy of 0.12 eV for perchlorate-doped PIN, with intercept value for T_0 and K_0 1.7×10^8 K and 9.3×10^{10} S cm⁻¹ K^{-1/2}, respectively, depicting a 3D conduction indicating more number of intrinsic charge transporter at room temperature. Arrhenius and Mott plots were observed to be fitted for variable hopping quasi 1D model in case of self-doped 5-PINC [15]. Temperature dependence conductivity of DNA-decorated PIN nanowires (diameter 19 nm) was described by Arrhenius model following the equation: $\ln G = \ln G_0 - (T_0/T)^\beta$ for 1D and 2D PIN structure $\beta = 1$ and $1/2$ were expected. On heating and cooling (233–373 K), no major hysteresis (only between 1 and 2%) was witnessed in the plot between G (conductance at zero bias) and T values was observed signifying the thermal stability of the composite material [23]. E_a values (Arrhenius

equation) from the slope were found to be of 0.24 eV which was comparably higher than PPY, PTH, PANI, etc., thus, leading to low conductivity of PIN-perchlorate. High E_a values suggest the presence of few intrinsic charge carriers in the polymer matrix at lower temperature. Similarly, the decay length and fermi level energy were comparable to PPY and were obeyed at higher temperature and support the variable range hopping mechanism [75] and supported more by Mott's equation compared to Arrhenius equation. One thing is to be noted that the studies should be carried at low temperature so as to understand the detailed charge transfer mechanism.

Conclusion

From the detail study done, the group had inferred that the PIN's electrical and electrochemical properties are widely affected by the method via which it is synthesized apart various factors including particle shape, size, dispersity along with solvent type, pH, temperature, etc. It was observed that the electrochemical performance of PIN decreases gradually with an increase of the scan rate and current density, which certainly can be attributed to the electrolytic ions diffusing and migrating into the active materials at low scan rates. This is because, at higher rates of scan, the diffusion effect limits the migration of the electrolytic ions and causing some active surface areas to become inaccessible for the charge storage; also this brings higher resistance in the electrodes. Studies suggest that the current response for the specific electrode material upsurges with increasing scan rate, attributed to variation in the thickness of the material layer formed at the electrode–electrolyte interface, which help in improved diffusion of the electrolyte into the bulk material thus causing higher current retort. It is suggested that optimum amount of PIN, increase active surface area, improved mesoporosity, and eases of the electrode–electrolyte interaction, and enhances interlayer charge carriage due to intercalation of conducting PIN in the matrix. Thus, concentration of PIN has a possible impression not only on the morphology but on thermal properties and electrochemical behaviour also. Easy diffusion of the electrolytic ions with a shorter diffusion route is favourably permitted with 3D design, this leading to greater charge discharge rates and a greater specific capacitance. Thus, from the studies, it can be extracted that enhanced capacitances (specific, gravimetric, and volumetric) and charge transport can be attributed to, edge effect, low-energy bandgap, layered porous assembly, particle size, geometrical organization, and electronic exchanges between the redox states (which are pH sensitive and pH dependent).

Thus, it can be concluded that hybrid PIN composites (binary or ternary composites) can be proved as a convincing

candidate for future generation supercapacitor application. However, like other CPs, PIN is also suffered with certain limitation, viz., instability, mechanical strain over long cycles, and material degradation, which limits its polymerization and storage properties, and therefore, green and competent methods of polymerization and judicious assortment of components for hybrid composite fabrication could be a key in this direction.

Acknowledgements Authors are thankful to all the publishers (ACS, RSC, Springer, Elsevier, Science Direct, etc.) to permit the reuse of figures and scheme in this review articles.

Open Access This article is distributed under the terms of the Creative Commons Attribution 4.0 International License (<http://creativecommons.org/licenses/by/4.0/>), which permits unrestricted use, distribution, and reproduction in any medium, provided you give appropriate credit to the original author(s) and the source, provide a link to the Creative Commons license, and indicate if changes were made.

References

- Omar, N., Gualous, H., Salminen, J., Mulder, G., Samba, A., Firouz, Y., Monem, M.A., Van den Bossche, P., Van Mierlo, J.: Electrical double-layer capacitors: evaluation of ageing phenomena during cycle life testing. *J. Appl. Electrochem.* **44**(4), 509–522 (2013). <https://doi.org/10.1007/s10800-013-0640-4>
- Ramya, R., Sivasubramanian, R., Sangaranarayanan, M.V.: Conducting polymers-based electrochemical supercapacitors—progress and prospects. *Electrochim. Acta* **101**, 109–129 (2013). <https://doi.org/10.1016/j.electacta.2012.09.116>
- Senthilkumar, S.T., Selvan, R.K., Lee, Y.S., Melo, J.S.: Electric double layer capacitor and its improved specific capacitance using redox additive electrolyte. *J. Mater. Chem. A* **1**(4), 1086–1095 (2013). <https://doi.org/10.1039/c2ta00210h>
- Inzelt, G.: Conducting polymers: past, present, future. *J. Electrochem. Sci. Eng.* **8**(1), 3–37 (2018). <https://doi.org/10.5599/jese.448>
- Mudila, H., Rana, S., Zaidi, M.G.H.: Supercritical CO₂ aided polyindole-graphene nanocomposites for high power density electrode. *Adv. Mater. Lett.* **8**(3), 269–275 (2017). <https://doi.org/10.5185/amlett.2017.7018>
- Tebyetekerwa, M., Yang, S., Peng, S., Xu, Z., Shao, W., Pan, D., Ramakrishna, S., Zhu, M.: Unveiling polyindole: freestanding as-electrospun polyindole nanofibers and polyindole/carbon nanotubes composites as enhanced electrodes for flexible all-solid state supercapacitors. *Electrochim. Acta* **247**, 400–409 (2017). <https://doi.org/10.1016/j.electacta.2017.07.038>
- Gao, Y.: Graphene and polymer composites for supercapacitor applications: a review. *Nanoscale Res. Lett.* **12**, 387 (2017). <https://doi.org/10.1186/s11671-017-2150-5>
- Phasuksom, K., Sirivat, A.: Synthesis of nano-sized polyindole via emulsion polymerization and doping. *Synth. Met.* **219**, 142–153 (2016). <https://doi.org/10.1016/j.synthmet.2016.05.033>
- Chhattise, P., Handore, K., Horne, A., Mohite, K., Chaskar, A., Dallavalle, S., Chabukswar, V.: Synthesis and characterization of polyindole and its catalytic performance study as a heterogeneous catalyst. *J. Chem. Sci.* **128**(3), 467–475 (2016). <https://doi.org/10.1007/s12039-016-1040-1>
- Pandey, P.C., Prakash, R.: Electrochemical synthesis of polyindole and its evaluation for rechargeable battery applications. *J. Electrochem. Soc.* **145**(3), 999–1003 (1998). <https://doi.org/10.1149/1.1838377>
- Tiwari, M., Kumar, A., Umre, H.S., Prakash, R.: Microwave-assisted chemical synthesis of conducting polyindole: study of electrical property using Schottky junction. *J. Appl. Polym. Sci.* **132**, 27 (2015). <https://doi.org/10.1002/app.42192>
- Ramesan, M.T.: Synthesis and characterization of magnetoelectric nanomaterial composed of Fe₃O₄ and polyindole. *Adv. Polym. Technol.* **32**(3), 1–9 (2013). <https://doi.org/10.1002/adv.21362>
- Jayakrishnan, P., Ramesan, M.T.: Synthesis, characterization, electrical conductivity and material properties of magnetite/polyindole/poly(vinyl alcohol) blend nanocomposites. *J. Inorgan. Organomet Polym Mater.* **27**(1), 323–333 (2017). <https://doi.org/10.1007/s10904-016-0474-8>
- Cai, Z.J., Zhang, Q., Song, X.Y.: Improved electrochemical performance of polyindole/carbon nanotubes composite as electrode material for supercapacitors. *Electron. Mater. Lett.* **12**(6), 830–840 (2016). <https://doi.org/10.1007/s13391-016-6190-2>
- Abthagir, P.S., Saraswathi, R.: Charge transport and thermal properties of polyindole, polycarbazole and their derivatives. *Thermochim. Acta* **424**, 25–35 (2004). <https://doi.org/10.1016/j.tca.2004.04.028>
- Bethany M.: Surge of green: a sustainable approach to conductive polymers. *Undergr. Rev.* **3**, 161–167 (2007). <https://core.ac.uk/download/pdf/48824622.pdf> (Last accessed on 02 June 2019)
- Zhou, W., Xu, J.: Progress in conjugated polyindoles: synthesis, polymerization mechanisms, properties, and applications. *Polym. Rev.* **57**(2), 248–275 (2016). <https://doi.org/10.1080/15583724.2016.1223130>
- Soylu, O., Uzun, S., Can, M.: The investigation of acid effect on chemical polymerization of indole. *Colloid Polym. Sci.* **289**(8), 903–909 (2011)
- Giribabu, K., Manigandan, R., Suresh, R., Vijayalakshmi, L., Stephen, A., Narayanan, V.: Polyindole nanowires: synthesis characterization and electrochemical sensing property. *Chem. Sci. Trans.* **2**(S1), S13–S16 (2013). <https://doi.org/10.7598/cst2013.2>
- Wenming, Y., Yang, C., Xiaoling, X., Zhiping, Z., Lukuan, L., Wanzhen, X.: Preparation of indole surface molecularly imprinted polymer by atom transfer radical emulsion polymerization and its adsorption performance. *J. Mater. Res.* **28**(19), 2666–2676 (2013). <https://doi.org/10.1557/jmr.2013.256>
- Kumar, A., Kumar, V., Kumar, M., Awasthi, K.: Synthesis and characterization of hybrid PANI/MWCNT nanocomposites for EMI applications. *Polym. Compos.* (2017). <https://doi.org/10.1002/pc.24418>
- Elango, M., Deepa, M., Subramanian, R., Musthafa, A.M.: Synthesis, characterization, and antibacterial activity of polyindole/Ag–CuO nanocomposites by reflux condensation method. *Polym. Plast. Technol. Eng.* **57**(14), 1440–1451 (2017). <https://doi.org/10.1080/03602559.2017.1410832>
- Hassanien, R., Al-Hinai, M., Al-Said, S.A.F., Little, R., Siller, L., Wright, N.G., Houlton, A., Horrocks, B.R.: Preparation and characterization of conductive and photoluminescent DNA-templated polyindole nanowires. *ACS Nano.* **4**(4), 2149–2159 (2010). <https://doi.org/10.1021/nn9014533>
- Zhijiang, C., Guang, Y.: Synthesis of polyindole and its evaluation for Li-ion battery applications. *Synth. Met.* **160**, 1902–1905 (2010). <https://doi.org/10.1016/j.synthmet.2010.07.007>
- Chagas, G.R., Darmanin, T., Guittard, F.: Nanostructured superhydrophobic films synthesized by electrodeposition of fluorinated polyindoles. *Beilstein J. Nanotechnol.* **6**, 2078–2087 (2015). <https://doi.org/10.3762/bjnano.6.212>
- Berkes, B.B., Bandarenka, A.S., Inzelt, G.: Electropolymerization: further insight into the formation of conducting polyindole thin films. *J. Phys. Chem. C* **119**(4), 1996–2003 (2015). <https://doi.org/10.1021/jp512208s>

27. Arjomandi, J., Nematollahi, D., Amani, A.: Enhanced electrical conductivity of polyindole prepared by electrochemical polymerization of indole in ionic liquids. *J. Appl. Polym. Sci.* **131**(40094), 1–5 (2014). <https://doi.org/10.1002/app.40094>
28. Sarac, A.S., Ozkara, S.: In-situ spectroelectrochemical investigation of indole polymerization. *Int. J. Polym. Mater. Polym. Biomater.* **53**(7), 587–599 (2004). <https://doi.org/10.1080/00914030490461702>
29. Xu, J., Hou, J., Zhou, W., Nie, G., Pu, S., Zhang, S.: ^1H NMR spectral studies on the polymerization mechanism of indole and its derivatives. *Spectrochim. Acta Part A.* **63**, 723–728 (2006). <https://doi.org/10.1016/j.saa.2005.06.025>
30. Singh, V., Chauhan, D.C., Pandey, P.C.: A comparative study on electrochemical synthesis of carboxylic acid substituted indoles and their application in selective oxidation of dopamine. In: IEEE SENSORS 2009 conference. Christchurch, New Zealand. 1140–1145. (2009) <https://doi.org/10.1109/icsens.2009.5398578>
31. Cai, Z., Yang, G.: Synthesis of polyindole and its evaluation for Li-ion battery applications. *Synth. Met.* **160**(17–18), 1902–1905 (2010). <https://doi.org/10.1016/j.synthmet.2010.07.007>
32. Mudila, H., Rana, S., Zaidi, M.G.H., Alam, S.: Polyindole/graphene oxide nanocomposites: the novel material for electrochemical energy storage. *Full. Nanotub. Carbon Nanostruct.* **23**(1), 20–26 (2013). <https://doi.org/10.1080/1536383x.2013.787604>
33. Majumder, M., Choudhary, R.B., Thakur, A.K., Rout, C.S., Gupta, G.: Rare earth metal oxide (RE_2O_3 ; RE = Nd, Gd, and Yb) incorporated polyindole composites: gravimetric and volumetric capacitive performance for supercapacitor applications. *New J. Chem.* **42**(7), 5295–5308 (2018). <https://doi.org/10.1039/c8nj00221e>
34. Raj, R.P., Ragupathy, P., Mohan, S.: Remarkable capacitive behavior of a Co_3O_4 -polyindole composite as electrode material for supercapacitor applications. *J. Mater. Chem. A* **3**(48), 24338–24348 (2015). <https://doi.org/10.1039/c5ta07046e>
35. Handore, K.N., Bhavsar, S.V., Pande, N., Chhattise, P.K., Sharma, S.B., Dallavalle, S., Gaikwad, V., Mohite, K.C., Chabukswar, V.V.: Polyindole-ZnO nanocomposite: synthesis, characterization and heterogeneous catalyst for the 3,4-dihydropyrimidinone synthesis under solvent-free conditions. *Polym. Plast. Technol. Eng.* **53**(7), 734–741 (2014). <https://doi.org/10.1080/03602559.2013.877930>
36. Khan, A.A., Khan, M.Q., Hussain, R.: Determination of Cd^{2+} in aqueous solution using polyindole-Ce(IV) vanadophosphate conductive nanocomposite ion-selective membrane electrode. *Mater. Res. Express* **4**(095024), 1–15 (2017). <https://doi.org/10.1088/2053-1591/aa8920>
37. Majumder, M., Choudhary, R.B., Koiry, S.P., Thakur, A.K., Kumar, U.: Gravimetric and volumetric capacitive performance of polyindole/carbon black/MoS₂ hybrid electrode material for supercapacitor applications. *Electrochim. Acta* **248**, 98–111 (2017). <https://doi.org/10.1016/j.electacta.2017.07.107>
38. Zhou, X., Chen, Q., Wang, A., Xu, J., Wu, S., Shen, J.: Bamboo-like composites of V_2O_5 /polyindole and activated carbon cloth as electrodes for all-solid-state flexible asymmetric supercapacitors. *ACS Appl. Mater. Interfaces.* **8**(6), 3776–3783 (2016). <https://doi.org/10.1021/acsami.5b10196>
39. Joshi, L., Singh, A.K., Prakash, R.: Polyindole/carboxylated-multiwalled carbon nanotube composites produced by in situ and interfacial polymerization. *Mater. Chem. Phys.* **135**(1), 80–87 (2012). <https://doi.org/10.1016/j.matchemphys.2012.04.026>
40. Bhagat, D.J., Dhokane, G.R.: AC conductivity investigation of polyindole/poly(vinyl acetate) composites. *J. Mater. Sci.* **27**(11), 11790–11797 (2016). <https://doi.org/10.1007/s10854-016-5319-2>
41. Park, I.H., Kwon, S.H., Choi, H.J.: Emulsion-polymerized polyindole nanoparticles and their electrorheology. *J. Appl. Polym. Sci.* **135**(25), 1–9 (2018). <https://doi.org/10.1002/app.46384>
42. Sarac, A.S., Ozkara, S., Sezer, E.: Electroco-polymerization of indole and thiophene: conductivity-peak current relationship and in situ spectroelectrochemical investigation of soluble co-oligomers. *Int J Polym Anal Charact* **8**(6), 395–409 (2003). <https://doi.org/10.1080/714975024>
43. Zhijiang, C., Ruihan, Z., Xingjuan, S.: Preparation and characterization of polyindole nanofibers by electrospinning method. *Synth. Met.* **162**(23), 2069–2074 (2012). <https://doi.org/10.1016/j.synthmet.2012.09.019>
44. Wu, J., Zhou, W., Jiang, F., Chang, Y., Zhou, Q., Li, D., Ye, G., Li, C., Nie, G., Xu, J., Li, T., Du, Y.: Three-dimensional porous carbon derived from polyindole hollow nanospheres for high-performance supercapacitor electrode. *ACS Appl. Energy Mater.* (2018). <https://doi.org/10.1021/acsaem.8b00722>
45. Zhou, W., Huang, D., Ma, X., Xu, J., Jiang, F., Lu, B., Zhu, D.: Porous poly(5-cyanoindole) electrode with high capacitance. *Adv Mater Res* **1053**, 235–239 (2014). <https://doi.org/10.4028/www.scientific.net/AMR.1053.235>
46. Ma, X., Zhou, W., Mo, D., Hou, J., Xu, J.: Effect of substituent position on electrodeposition, morphology, and capacitance performance of polyindole bearing a carboxylic group. *Electrochim. Acta* **176**, 1302–1312 (2015). <https://doi.org/10.1016/j.electacta.2015.07.148>
47. Wang, W., Ren, G., Wang, M., Liu, Y., Wu, S., Shen, J.: A novel composite for energy storage devices: core-shell MnO_2 /polyindole nanotubes supported on reduced graphene oxides. *J. Mater. Sci.: Mater. Electron.* **29**(7), 5548–5560 (2018). <https://doi.org/10.1007/s10854-018-8523-4>
48. Ozkazanc, H.: Characterization and charge transfer mechanism of PIN-CdSe nanocomposites. *Polym. Compo.* **37**(10), 1–9 (2015). <https://doi.org/10.1002/pc.23503>
49. Khati, K., Joshi, I., Bisht, A., Zaidi, M.G.H.: Haemoglobin/polyindole composites: the novel material for electrochemical supercapacitors. *Bull. Mater. Sci.* **42**(1), 1–6 (2019). <https://doi.org/10.1007/s12034-018-1700-5>
50. Verma, C.J., Pandey, R.K., Prakash, R.: In situ one step synthesis of Fe inserted octaethylporphyrin/polyindole: a multifunctional hybrid material with improved electrochemical and electrical properties. *Mater. Sci. Eng. B* **227**, 80–88 (2018). <https://doi.org/10.1016/j.mseb.2017.10.015>
51. Majumder, M., Choudhary, R.B., Thakur, A.K.: Hemispherical nitrogen-doped carbon spheres integrated with polyindole as high performance electrode material for supercapacitor applications. *Carbon* **142**, 650–661 (2019). <https://doi.org/10.1016/j.carbon.2018.10.089>
52. Rajasudha, G., Shankar, H., Thangadurai, P., Boukos, N., Narayanan, V., Stephen, A.: Preparation and characterization of polyindole-ZnO composite polymer electrolyte with LiClO_4 . *Ionics* **16**, 839–848 (2010). <https://doi.org/10.1007/s11581-010-0472-8>
53. Rajasudha, G., Nancy, A.P., Thangadurai, P., Boukos, N., Narayanan, V., Stephen, A.: Synthesis and characterization of polyindole-NiO-based composite polymer electrolyte with LiClO_4 , international journal of polymeric materials and polymeric. *Biomaterials* **60**(11), 877–892 (2011). <https://doi.org/10.1080/00914037.2010.551367>
54. Rajasudha, G., Jayan, L.M., Lakshmi, D.D., Thangadurai, P., Boukos, N., Narayanan, V., Stephen, A.: Polyindole-CuO composite polymer electrolyte containing LiClO_4 for lithium ion polymer batteries. *Polym. Bull.* **68**, 181–196 (2012). <https://doi.org/10.1007/s00289-011-0548-2>
55. Rajasudha, G., Lakshmi, D.D., Thangadurai, P., Boukos, N., Narayanan, V., Stephen, A.: Preparation and characterization of polyindole-iron oxide composite polymer electrolyte containing LiClO_4 . *Polym. Plast. Technol. Eng.* **51**(3), 225–230 (2012). <https://doi.org/10.1080/03602559.2011.618159>

56. Oraon, R., Adhikari, A.D., Tiwari, S.K., Bhattacharyya, S., Nayak, G.C.: Hierarchical self-assembled nanoclay derived mesoporous CNT/polyindole electrode for supercapacitors. *RSC Adv.* **6**, 64271–64284 (2016). <https://doi.org/10.1039/C6RA12938B>
57. Tebyetekerwa, M., Xu, Z., Li, W., Wang, X., Marriam, I., Peng, S., Ramkrishna, S., Yang, S., Zhu, M.: Surface self-assembly of functional electroactive nanofibers on textile yarns as a facile approach toward super flexible energy storage. *ACS Appl. Energy Mater.* **1**(2), 377–386 (2017). <https://doi.org/10.1021/acsaem.7b00057>
58. Zhou, X., Wang, A., Pan, Y., Yu, C., Zou, Y., Zhou, Y., Chen, Q., Wu, S.: Facile synthesis of a Co_3O_4 @carbon nanotubes/polyindole composite and its application in all-solid-state flexible supercapacitors. *J. Mater. Chem. A* **3**(24), 13011–13015 (2015). <https://doi.org/10.1039/c5ta01906k>
59. Purty, B., Choudhary, R.B., Biswas, A., Udayabhanu, G.: Chemically grown mesoporous f-CNT/ α - MnO_2 /PIIn nanocomposites as electrode materials for supercapacitor application. *Polym. Bull.* **76**(4), 1619–1640 (2019). <https://doi.org/10.1007/s00289-018-2458-z>
60. Ramesan, M.T., Anjitha, T., Parvathi, K., Anil kumar, T., Mathew, G.: Nano zinc ferrite filler incorporated polyindole/poly(vinyl alcohol) blend: preparation, characterization, and investigation of electrical properties. *Adv. Polym. Technol.* **37**(8), 3639–3649 (2018). <https://doi.org/10.1002/adv.22148>
61. Bhagat, D.J., Dhokane, G.R.: Electro-optical properties of one pot synthesized polyindole in the presence of poly(vinyl acetate). *Electron. Mater. Lett.* **11**(3), 346–351 (2015). <https://doi.org/10.1007/s13391-015-4426-1>
62. Eraldemir, O., Sari, B., Gok, A., Unal, H.I.: Synthesis and characterization of polyindole/poly(vinyl acetate) conducting composites. *J. Macromol. Sci. Part A Pure Appl. Chem.* **45**(3), 205–211 (2008). <https://doi.org/10.1080/10601320701839890>
63. Gergin, I., Gokceoren, A.T., Sarac, A.S.: Synthesis and electrochemical investigation of polyindole based fiber as sensor electrode by EIS method. *Fibers Polym.* **16**(7), 1468–1477 (2015). <https://doi.org/10.1007/s12221-015-5144-x>
64. Kuo, C.W., Wu, T.Y., Fan, S.C.: Applications of poly(indole-6-carboxylic acid-co-2,2'-bithiophene) films in high-contrast electrochromic devices. *Coatings* **8**(3), 102 (2018). <https://doi.org/10.3390/coatings8030102>
65. Gupta, B., Chauhan, D.S., Prakash, R.: Controlled morphology of conducting polymers: formation of nanorods and microspheres of polyindole. *Mater. Chem. Phys.* **120**, 625–630 (2010). <https://doi.org/10.1016/j.matchemphys.2009.12.026>
66. Zhijiang, C., Xingjuan, S., Yanan, F.: Electrochemical properties of electrospun polyindole nanofibers as a polymer electrode for lithium ion secondary battery. *J. Power Sour.* **277**, 53–59 (2013). <https://doi.org/10.1016/j.jpowsour.2012.10.081>
67. Jayakrishnan, P., Pradyumnan, P.P., Ramesan, M.T.: Thermal and electrical properties of polyindole/magnetite nanocomposites. *Chem. J. Am. Inst. Chem.* **89**(1), 27–32 (2016)
68. Rajasudha, G., Narayanan, V., Stephen, A.: Effect of iron oxide on ionic conductivity of polyindole based composite polymer electrolytes. *Adv. Mater. Res.* **584**, 536–540 (2012). <https://doi.org/10.4028/www.scientific.net/amr.584.536>
69. Ma, X., Zhou, W., Mo, D., Wan, Z., Xu, J.: Capacitance comparison of poly(indole-5-carboxylic acid) in different electrolytes and its symmetrical supercapacitor in HClO_4 aqueous electrolyte. *Synth. Met.* **203**, 98–106 (2015). <https://doi.org/10.1016/j.synthmet.2015.02.025>
70. Berkes, B.B., Inzelt, G.: Electrochemical nanogravimetric studies on the electropolymerization of indole and on polyindole. *Electrochim. Acta* **122**, 11–15 (2014). <https://doi.org/10.1016/j.electacta.2013.06.035>
71. Wadatkar, N.S., Waghuley, S.A.: Complex optical studies on conducting polyindole as-synthesized through chemical route. *Egypt. J. Basic Appl. Sci.* **2**(1), 19–24 (2015). <https://doi.org/10.1016/j.ejbas.2014.12.006>
72. Nateghi, M.R., Frahmmand, S., Mirjalili, G.: Optical constants of electrochemically synthesized polyindole and poly(5-carboxylic acid indole). *Polym. Sci. Ser. A* **56**(4), 459–464 (2014). <https://doi.org/10.1134/s0965545x14040117>
73. Rejania, P., Beena, B.: Structural and optical properties of polyindole-manganese oxide nanocomposite. *Indian J. Adv. Chem. Sci.* **2**(3), 244–248 (2013)
74. Bhagat, D.J., Bajaj, N.S., Dhokane, G.R.: Electro-optical properties of poly(vinyl acetate)/polyindole composite film. *Am Inst Phys* **1728**, 020171 (2016). <https://doi.org/10.1063/1.4946222>
75. Abthagir, P.S., Dhanalakshmi, K., Saraswathi, R.: Thermal studies on polyindole and polycarbazole. *Synth. Met.* **93**, 1–7 (1998)
76. Wang, W., Wu, S.: A new ternary composite based on carbon nanotubes/polyindole/graphene with preeminent electrocapacitive performance for supercapacitors. *Appl. Surf. Sci.* **396**, 1360–1367 (2017). <https://doi.org/10.1016/j.apsusc.2016.11.167>
77. Li, D., Zhu, D., Zhou, W., Ma, X., Zhou, Q., Ye, G., Xu, J.: Porous multilayered films based on poly(3,4-ethylenedioxythiophene) and poly(indole-5-carboxylic acid) and their capacitance performance. *Int. J. Electrochem. Sci.* **12**, 2741–2753 (2017). <https://doi.org/10.20964/2017.04.65>
78. Tebyetekerwa, M., Wang, X., Marriam, I., Dan, P., Yang, S., Zhu, M.: Green approach to fabricate polyindole composite nanofibers for energy and sensor applications. *Mater. Lett.* **209**, 400–403 (2017). <https://doi.org/10.1016/j.matlet.2017.08.062>

Publisher's Note Springer Nature remains neutral with regard to jurisdictional claims in published maps and institutional affiliations.